

On the gravitational partition function under volume constraints

Shan-Ping Wu,^{a,b} Peng Cheng,^c Shao-Wen Wei^{1a,b}

^a*Lanzhou Center for Theoretical Physics, Key Laboratory of Theoretical Physics of Gansu Province, and Key Laboratory of Quantum Theory and Applications of MoE, Lanzhou University, Lanzhou, Gansu 730000, China*

^b*Institute of Theoretical Physics & Research Center of Gravitation, Lanzhou University, Lanzhou 730000, China*

^c*Center for Joint Quantum Studies and Department of Physics, School of Science, Tianjin University, Tianjin 300350, China*

E-mail: 120220908841@lzu.edu.cn, p.cheng.nl@outlook.com,
weishw@lzu.edu.cn

ABSTRACT: The Euclidean action serves as a bridge between gravitational thermodynamics and the partition function. In this work, we further examine the gravitational partition function under a fixed volume constraint, extending the fixed volume on-shell geometry in the massless case. Moving beyond this massless configuration, we construct solutions with nonzero mass functions, leading to a new class of volume-constrained Euclidean geometries (VCEGs). The VCEG contains both a boundary and a horizon, and its Euclidean action is determined solely by the contribution from the horizon. However, further investigation suggests that this boundary appears to be artificially constructed and can be extended, giving rise to the extended VCEGs. These geometries feature two horizons, each with a conical singularity, and their action is given by one-quarter of the sum of the areas of the two horizons. In general, the conical singularities on both horizons cannot be simultaneously removed, except at a critical mass $m = m^*$, which defines the critical extended VCEG. Configurations with conical singularities are interpreted as constrained gravitational instantons. An analysis of their contributions to the partition function and topology reveals a close analogy between the extended VCEGs and the Euclidean Schwarzschild-de Sitter static patch, suggesting that the volume constraint effectively plays a role akin to that of a cosmological constant in semiclassical quantum gravity.

KEYWORDS: Euclidean action, constrained instantons, de Sitter black hole

¹Corresponding author

Contents

1	Introduction	1
2	Metric solutions in finite volume	5
2.1	Case I: $p'(r) = 0$	6
2.2	Case II: $\rho(r) = 0$	8
3	Euclidean formalism and Iyer-Wald entropy	10
4	Geometric contributions to the Euclidean action	13
4.1	General considerations	13
4.2	The four-dimensional case	15
5	Extension of the volume-constrained Euclidean geometry	17
5.1	The four-dimensional case	18
5.2	Higher-dimensional extension	22
6	Euclidean geometry as constrained instantons	23
6.1	Constrained instantons in gravity	24
6.2	Ensemble interpretation and quantum decay rate	27
7	Conclusion and discussion	29
A	Special Case: three dimensions	31

1 Introduction

Black holes occupy a central place in modern theoretical physics, serving as a natural arena where gravity and quantum theory intersect. Seminal work has revealed that black holes emit radiation, now known as Hawking radiation [1], and exhibit a range of thermodynamic properties [2–5]. In particular, they obey analogs of the four laws of thermodynamics [6–8] and can undergo phase transitions [9–12], placing them on a similar footing with ordinary thermodynamic systems. Yet black hole thermodynamics also presents profound departures from conventional thermodynamics. Most notably, the entropy of a black hole is not directly related to its volume but instead scales with the area of its event horizon. This area law strongly suggests that the microscopic degrees of freedom of gravity are encoded on lower-dimensional surfaces, pointing toward the holographic nature of gravitational systems [13–16].

Along the way to black hole thermodynamics, the Euclidean path integral has proven to be a powerful and successful approach [4, 5]. Within the framework of thermal quantum field theory, the gravitational partition function can be formulated as a path integral,

$$\mathcal{Z}_\beta = \int [\mathcal{D}g] \exp(-I_E[g]), \quad (1.1)$$

where $I_E[g]$ denotes the Euclidean gravitational action evaluated on a metric g , and β represents the inverse temperature associated with the Euclidean time periodicity. The path integral is taken over all metrics that are periodic in β and satisfy the appropriate asymptotic fall-off conditions. In practice, evaluating this path integral is highly nontrivial. When fluctuations are small, however, the saddle-point approximation provides an effective approach, yielding

$$\mathcal{Z} \simeq \exp(-I_E[g_{\text{on-shell}}]), \quad (1.2)$$

where $g_{\text{on-shell}}$ denotes a metric that satisfies the classical equations of motion, i.e., an on-shell geometry. From this partition function, one can systematically derive thermodynamic quantities such as energy, entropy, and free energy. When the Einstein–Hilbert action with a positive cosmological constant is considered, the Euclidean section obtained by Wick rotating the Lorentzian de Sitter (dS) static patch provides an on-shell saddle. Its contribution to the partition function is given by

$$\mathcal{Z} \simeq \exp(\mathcal{A}_H/(4\hbar G)), \quad (1.3)$$

where \mathcal{A}_H denotes the area of the dS horizon. For geometries satisfying the field equations (or, more precisely, the Hamiltonian and momentum constraints), the corresponding action is typically determined by contributions from horizons or boundaries. This feature has been discussed extensively in the literature [17–20] and will also be reviewed in Sec. 3. In the Euclidean de Sitter (dS) static patch, where the geometry is smooth and possesses no boundary other than the regularized horizon, the Euclidean action is proportional to the horizon area. While this structure is manifest within the gravitational path integral, its physical interpretation remains less transparent. Viewed from the Euclidean static patch, the geometry is compact and boundaryless. It can be formally regarded as having an artificial internal spherical boundary of radius R_B , with the limit $R_B \rightarrow 0$ [19, 27]. In this limit, the corresponding Brown–York Hamiltonian H_{BY} vanishes. The partition function can then be expressed as a trace over the Hilbert space states, $\mathcal{Z} = \text{Tr} \exp(-\beta H_{\text{BY}}) = \text{Tr} I$. Hence, the dimension of the Hilbert space is directly given by the partition function, and is therefore proportional to $\exp(\mathcal{A}_H/4\hbar G)$. This idea was advocated by Fischler [21] and Banks [22], who argued that, since the sphere partition function is an integral unconstrained by any boundary conditions, the quantity \mathcal{Z}_β must represent the dimension of the Hilbert space of all states in the theory describing a spatial volume. Furthermore, from a holographic perspective, developments in dS/CFT suggest that this entropy reflects the number of quantum gravitational degrees of freedom associated with the cosmological horizon [23–26].

More recently, these ideas have been extended to the study of Einstein gravity under a fixed-volume constraint, with the corresponding partition function investigated in Ref. [27].

In this framework, the on-shell geometry is compact, featuring a horizon but no boundary, similar to pure dS spacetime. The contribution of such an on-shell geometry to the Euclidean action can be interpreted as the dimension of the Hilbert space of a spatial region with the topology of a ball and fixed proper volume, given precisely by one-quarter of the horizon area. Extensions to higher-derivative theories have also been explored, including massive gravity [28] and Lovelock gravity [29], where the strict area law is replaced by the Wald entropy [30].

In the fixed-volume framework, the on-shell gravitational solutions discussed in Ref. [27] were obtained by analyzing the Tolman-Oppenheimer-Volkoff (TOV) equation [31–34] with a vanishing mass function, without accounting for nonzero mass functions or energy densities. In this work, we extend beyond the massless configuration and construct solutions with nonzero mass functions, thereby forming a broader class of volume-constrained Euclidean geometries (VCEGs). To understand the relevance of such configurations, it is useful to note the following points. First, geometries with a nonzero constant mass should still be regarded as admissible solutions of the volume-constrained gravitational field equations, and their contribution to the path integral remains physically relevant. This point is crucial: without the volume constraint, a vanishing mass function yields only the trivial flat solution, while a nonzero mass function can give rise to meaningful solutions, such as the Schwarzschild black hole, demonstrating the significance of considering nonzero mass functions within this framework. Second, to account for possible excitations of the energy density under the volume constraint, we introduce a simple model to study how the mass function or matter affects the resulting on-shell spacetime. Interestingly, the behavior of configurations with a vanishing mass function closely resembles that of the Euclidean de Sitter (dS) static patch, suggesting that when the mass function becomes nonzero, the corresponding on-shell geometry may develop features analogous to those of the static patch of a Euclidean Schwarzschild–de Sitter (SdS) black hole. As will be shown below, this expectation is indeed realized.

On the other hand, these volume-constrained solutions can also be interpreted as constrained gravitational instantons [35–38]. Although they are not vacuum solutions of the Einstein equations in the absence of a volume constraint, they provide nontrivial contributions to nonperturbative processes in quantum gravity. The volume parameter effectively labels different constraint sectors, so that the total gravitational partition function can be regarded as a sum over instantons with varying volumes. From this perspective, constrained instantons under fixed-volume conditions are expected to play a significant role in the path integral for the Einstein-Hilbert action. In the present work, however, we focus not on unconstrained Einstein gravity, but on Einstein gravity with a fixed-volume constraint and the corresponding VCEGs. We find that, in the case of a constant nonzero mass function, the VCEGs can be extended, and this extended geometry should be understood as a mass-constrained gravitational instanton. Indeed, in the dS case, the only genuinely smooth instantons are the Euclidean dS static patch and the Nariai geometry, whereas generic SdS configurations are naturally interpreted as constrained instantons with fixed mass [39, 40]. We further observe a close analogy between the extended VCEGs with nonzero mass functions and the SdS black hole.

We therefore regard the VCEGs with a nonzero mass function, or more precisely, the ex-

tended VCEGs, as playing an important role, much like the SdS black hole does in the study of gravitational instantons [39, 40]. As constrained instanton solutions, their contributions to the Euclidean action are physically significant. It is thus natural to further investigate how both the VCEGs and extended VCEGs contribute to the action and the corresponding partition function. To better analyze the contribution of geometries to the action, we employ the covariant phase space formalism [20, 30, 41–47] in the fixed-volume framework. This approach reveals that, for gravitational configurations satisfying the Hamiltonian and momentum constraints, the dominant contributions to the action arise from the horizon and the boundary. The horizon contribution reproduces the Wald entropy, while the boundary contribution typically corresponds to the energy. Importantly, this analysis is general and can be extended to covariant metric theories of gravity beyond Einstein gravity. Once the Euclidean action is obtained, we further analyze its role in the path integral, including the interpretation of ensembles and decay rates.

The main purpose of this work is to extend the class of metric solutions in Einstein gravity under a fixed-volume constraint and to investigate their geometric properties, contributions to the gravitational partition function, as well as the associated physical implications. The paper is organized as follows. In Sec. 2, we consider the TOV equation associated with the effective matter induced by the volume constraint, from which the VCEGs are obtained. In Secs. 3 and 4, using the covariant phase space formalism, we analyze the contributions of the VCEGs to the Euclidean action and show how the horizon and boundary terms encode the entropy and energy, respectively. In Sec. 5, through a suitable coordinate transformation, we analytically extend the VCEGs and examine their impact on the Euclidean action. In Sec. 6, we review the notion of constrained gravitational instantons, interpret the extended VCEGs as mass-constrained instantons, and discuss their role in the gravitational partition function and the decay rates of the massless VCEGs. Finally, Sec. 7 summarizes our findings and comments on the close connection between the extended VCEGs and the SdS black hole.

Notation: Throughout this paper, we set $G = c = \hbar = 1$, unless otherwise stated. The numerically invariant Levi-Civita symbol is denoted by $\varepsilon_{a_1 \dots a_d}$, taking values 0, 1, or -1 . We also introduce

$$\epsilon_{a_1 \dots a_d} \equiv \sqrt{|g|} \varepsilon_{a_1 \dots a_d},$$

$$(d^n x)_{a_1 \dots a_{(d-n)}} \equiv \frac{1}{(d-n)! n!} \varepsilon_{a_1 \dots a_{(d-n)} a_{(d-n+1)} \dots a_d} dx^{a_{(d-n+1)}} \wedge \dots \wedge dx^{a_d}.$$

For simplicity we omit explicit references to the static patch. Unless stated otherwise, Euclidean dS spacetime and Euclidean SdS black hole are understood to refer exclusively to their respective static patches.

2 Metric solutions in finite volume

When a fixed spatial volume is imposed, the D -dimensional (or equivalently, $d+2$ -dimensional) Euclidean action of Einstein gravity can be written as

$$I_E = -\frac{1}{16\pi} \int_M \sqrt{g} R d^D x - \int d\tau \lambda(\tau) \left(\int_{\Sigma_\tau} \sqrt{\gamma} d^{D-1} x - V \right) - \frac{1}{8\pi} \int_{\partial M} \sqrt{h} K d^{D-1} x, \quad (2.1)$$

where the second term separates the integration over the manifold M into an integral along the Euclidean time τ direction and an integral over the spacelike slices Σ_τ for τ -constant. Here, γ denotes the determinant of the induced metric γ_{ab} on Σ_τ , and the Lagrange multiplier $\lambda(\tau)$ enforces the volume constraint, fixing the spatial volume V on each spacelike slice. The third term represents the Gibbons-Hawking-York boundary contribution, where h denotes the determinant of the induced metric h_{ab} on the boundary ∂M , and K is the trace of the extrinsic curvature. Varying this action with respect to the metric g^{ab} and the Lagrange multiplier $\lambda(\tau)$ yields the equations of motion,

$$R_{ab} - \frac{1}{2} g_{ab} R = \frac{8\pi\lambda}{N} \gamma_{ab}, \quad V = \int_{\Sigma_\tau} \sqrt{\gamma} d^{D-1} x, \quad (2.2)$$

where N is the lapse function, which can be written explicitly as $N = \sqrt{g/\gamma}$. In the spherically symmetric and static case, the field equations admit metric solutions [27],

$$ds^2 = \frac{1}{4R^2} (R^2 - r^2)^2 d\tau^2 + dr^2 + r^2 d\Omega_d^2, \quad V = \int_0^R r^{d+1} dr d\Omega_d. \quad (2.3)$$

The geometry admits a timelike Killing vector $\xi = \partial_\tau$ with surface gravity $\kappa = \sqrt{\nabla_a \xi_b \nabla^a \xi^b / 2} = 1$, which corresponds to an inverse temperature of period $\beta = 2\pi$. Since the manifold is compact and contains a horizon (at $r = R$) but no boundary, its contribution to the partition function is $\mathcal{Z} = \exp(\mathcal{A}/4)$, where \mathcal{A} denotes the horizon area ¹. However, the corresponding solution is characterized by a vanishing mass function $M(r) = 0$ and thus does not represent the most general case. In what follows, we will construct more general solutions.

As a starting point, we consider the gravitational field equations coupled to a perfect fluid, which take the form

$$R_{ab} - \frac{1}{2} g_{ab} R = 8\pi T_{ab}, \quad (2.4)$$

$$T_{ab} = -\rho(r) n_a n_b + p(r) \gamma_{ab}, \quad (2.5)$$

where $\rho(r)$ denotes the energy density of the perfect fluid, and $p(r)$ is the corresponding pressure. We adopt the spherically symmetric ansatz

$$ds^2 = N(r)^2 d\tau^2 + \left(1 - \frac{16\pi}{d\Omega_d} \frac{M(r)}{r^{d-1}} \right)^{-1} dr^2 + r^2 d\Omega_d^2, \quad (2.6)$$

¹For a detailed discussion, see Sec. 3.

where $M(r)$ denotes the mass function and $N(r)$ is the lapse function, both of which are to be determined. For convenience, and without loss of generality, we assume $N(r) > 0$. Because of spherical symmetry, the angular components of the field equations are equivalent. It therefore suffices to consider the $\tau\tau$ -component, the rr -component, and one representative angular component of Eq. (2.4). Thus, only three independent equations need to be analyzed. From $\tau\tau$ - and rr -components, one readily obtains

$$M'(r) = \rho(r) \Omega_d r^d, \quad (2.7)$$

$$N'(r) = -\frac{8\pi N(r)}{16\pi r M(r) - d\Omega_d r^d} \left((d-1)M(r) + r^{d+1}\Omega_d p(r) \right). \quad (2.8)$$

It is clear that, once the density $\rho(r)$ and pressure $p(r)$ are specified, Eqs. (2.7) and (2.8) uniquely determine the metric. In general, however, the resulting solution does not satisfy the angular components of the field equations. This implies that $\rho(r)$ and $p(r)$ are subject to an additional condition arising from the angular components of the field equations. When incorporated into Eqs. (2.7) and (2.8), this condition is exactly equivalent to the conservation of the energy-momentum tensor, $\nabla_a T^{ab} = 0$. Of these, only the r -component is nontrivial and reads,

$$(\rho(r) + p(r)) \frac{N'(r)}{N(r)} + p'(r) = 0. \quad (2.9)$$

Thus, for the three equations given by Eqs. (2.7), (2.8), and (2.9), there are four unknown functions: $N(r)$, $M(r)$, $\rho(r)$, and $p(r)$. By specifying one of these functions appropriately, or by imposing an additional suitable constraint, both the gravitational metric and the corresponding energy-momentum tensor can be determined.

When the volume constraint, Eq. (2.2), is imposed, a natural relation arises,

$$p(r) = \frac{\lambda}{N(r)}, \quad (2.10)$$

which fully determines the solutions. To proceed, imposing this relation simplifies Eq. (2.9), which becomes

$$\frac{\rho(r) p'(r)}{p(r)} = 0 \quad \text{or equivalently} \quad \frac{M'(r) N'(r)}{N(r)} = 0. \quad (2.11)$$

From this, we see that there are two possible types of solutions: first, the case $p'(r) = 0$, or equivalently $N'(r) = 0$; and second, the case $\rho(r) = 0$, or equivalently $M'(r) = 0$. These two cases correspond to distinct classes of solutions.

2.1 Case I: $p'(r) = 0$

In this case, we have $p'(r) = 0$, which is equivalent to $N'(r) = 0$. Consequently, Eqs. (2.7), (2.8), and (2.9) reduce to algebraic equations. The lapse function becomes constant, specifically $N(r) = N_0$, where N_0 is a constant. The corresponding metric solution reads

$$ds^2 = N_0^2 d\tau^2 + \frac{1}{1 - \frac{16\pi\rho_0}{d(d+1)} r^2} dr^2 + r^2 d\Omega_d^2, \quad (2.12)$$

with the energy density and pressure given by

$$\rho(r) = \rho_0, \quad p(r) = \frac{\lambda}{N_0}, \quad (2.13)$$

where

$$\rho_0 = -\frac{d+1}{d-1} \frac{\lambda}{N_0}. \quad (2.14)$$

When the constant energy density satisfies $\rho_0 > 0$, the metric is confined to the radial region $r \in [0, r_c]$, where

$$r_c = \sqrt{\frac{d(d+1)}{16\pi\rho_0}}. \quad (2.15)$$

At $r = r_c$, the metric appears to diverge; however, this is merely a coordinate singularity. Introducing a new radial coordinate η ,

$$\eta = \arcsin \left(\sqrt{\frac{16\pi\rho_0}{d(d+1)}} r \right), \quad (2.16)$$

the metric becomes manifestly regular,

$$ds^2 = N_0^2 d\tau^2 + \frac{d(d+1)}{16\pi\rho_0} (d\eta^2 + \sin^2 \eta d\Omega_d^2). \quad (2.17)$$

Note that $r \in [0, r_c]$ corresponds to $\eta \in [0, \pi/2]$. In the η coordinate, the geometry admits a natural extension, with $\eta \in [0, \pi]$. In this form, it is clear that the spatial section corresponds to a $(d+1)$ -sphere with volume,

$$V = \Omega_{d+1} \left(\frac{d(d+1)}{16\pi\rho_0} \right)^{(d+1)/2}, \quad (2.18)$$

and the full geometry is given by the product space $\mathbb{S}^1 \times \mathbb{S}^{d+1}$. If $\rho_0 < 0$, the spacetime is not confined to a finite radial region. By applying a coordinate transformation similar to the one discussed above, one finds that the spatial section becomes a hyperbolic space. Physically, even in the presence of the volume constraint, a negative energy density allows the spacetime to extend indefinitely.

Let us briefly examine the energy conditions. For the energy density and pressure specified in Eq. (2.13), one finds that if $\lambda < 0$, then

$$\rho = \rho_0 > 0, \quad \rho + p = \frac{2}{d+1} \rho_0, \quad \rho + (d+1)p = -d\rho_0 < 0, \quad \rho > |p|. \quad (2.19)$$

It then follows that the weak and dominant energy conditions are satisfied, while the strong energy condition is violated. However, in the present setup, the volume constraint has been effectively interpreted as a matter pressure. In fact, the additional excitation under consideration carries only energy and no pressure. Therefore, when $\lambda < 0$, all three standard energy conditions are actually satisfied.

2.2 Case II: $\rho(r) = 0$

In this case, we have $\rho(r) = 0$, which is equivalent to $M'(r) = 0$. Since the energy density vanishes, we have

$$\rho(r) = 0, \quad p(r) = \frac{\lambda}{N(r)}. \quad (2.20)$$

Equation (2.7) then implies that the function M takes a constant value. To avoid a naked singularity at $r = 0$, we assume this constant to be positive. For convenience, we parametrize it as

$$M(r) = \frac{d\Omega_d}{16\pi} m^{d-1}, \quad (2.21)$$

where m is a constant with the dimension of length, assumed to be non-negative. For clarity and consistency in the subsequent discussion, we refer to m as the mass parameter, and to M as the mass constant (or mass function). Under this parametrization, the metric ansatz (2.6) takes the form

$$ds^2 = N(r)^2 d\tau^2 + \left(1 - \frac{m^{d-1}}{r^{d-1}}\right)^{-1} dr^2 + r^2 d\Omega_d^2. \quad (2.22)$$

It is evident that for nonzero m , the requirement $g_{rr} > 0$ restricts the geometry to the region $r \geq m$. The remaining function $N(r)$ is then determined by Eq. (2.8), which becomes

$$N'(r) = \frac{d(d-1)m^{d-1}N(r) + 16\pi\lambda r^{d+1}}{2dr(r^{d-1} - m^{d-1})}. \quad (2.23)$$

Since we are considering the region $r \geq m$ and $N(r) \geq 0$, one immediately observes that if $\lambda > 0$, the function $N(r)$ is monotonically increasing. Consequently, $N(r)$ admits no zeros, and the geometry remains open. On the other hand, for $\lambda < 0$, the asymptotic behavior of the solution at large r is given by

$$N(r) \sim \lambda r^2 < 0, \quad (2.24)$$

which is incompatible with the positivity requirement. This implies that $N(r)$ must necessarily vanish at some finite radius greater than m , denoted by $r = r_c$. Substituting $r = r_c$ into Eq. (2.23), one finds $N'(r_c) < 0$. Therefore, for a continuous solution, $N(r)$ possesses a unique zero, and the physically admissible domain is restricted to the interval (m, r_c) . From Eq. (2.23), together with the condition $N(r_c) = 0$, one can solve for $N(r)$ as

$$N(r) = \frac{-8\pi\lambda m^2}{d} \sqrt{1 - \frac{m^{d-1}}{r^{d-1}}} C(r), \quad C(r) = \int_{m/r_c}^{m/r} \frac{1}{x^3 (1 - x^{d-1})^{3/2}} dx. \quad (2.25)$$

Note that $m \leq r \leq r_c$, so that the integration range in the second expression is constrained by $m/r_c \leq m/r \leq 1$. It is further worth noting that as $r \rightarrow m$, the integral behaves asymptotically as $C(r) \sim (1 - m/r)^{-1/2}$. Although this suggests a divergence, the prefactor in the expression for $N(r)$ precisely cancels this divergence, ensuring that $N(r)$ remains finite at $r = m$. Another singularity of interest arises in g_{rr} at $r = m$, which, as in the case discussed in Sec. 2.1, is merely a coordinate singularity and can be removed via an appropriate coordinate transformation.

One observes that the resulting geometry shares certain similarities with the global black hole geometry; however, there are crucial differences. In particular, although g^{rr} vanishes at $r = m$, the lapse function $g_{tt} = N(r)^2$ does not. Upon continuation to Lorentzian signature, the region $r < m$ would develop two timelike directions, one along the original time coordinate and the other along the radial direction. We therefore regard this sector as unphysical and do not extend the geometry into $r < m$. On the other side, the region $r > r_c$, where $N(r)$ becomes negative, cannot be analytically continued. Recall that the original definition $p(r) = \lambda/|N(r)|$ can be simplified to $p(r) = \lambda/N(r)$ under the assumption $N(r) > 0$. Once $N(r) < 0$, this assumption breaks down, Eq. (2.23) undergoes a substantial change, and the continuation of $N(r)$ no longer satisfies the field equations. Consequently, the spacetime under consideration is strictly restricted to the domain $m \leq r \leq r_c$.

By varying the Lagrange multiplier λ , one imposes the volume constraint. The corresponding constrained volume is obtained by integrating the spatial part of the metric over the radial interval from $r = m$ to $r = r_c$, yielding,

$$V = \Omega_d m^{d+1} \int_{m/r_c}^1 \frac{1}{(1-x^{d-1})^{1/2} x^{d+2}} dx. \quad (2.26)$$

It is straightforward to observe that, although the integrand exhibits a singularity at $x = 1$ (i.e., $r = m$), the divergence behaves as $(1-x)^{-1/2}$ and is therefore finite in the sense of the integral.

In the previous discussion, although we did not present the explicit form of the geometric solution, its behavior can be inferred from the analysis of the differential equations. In the following, we focus on the case $d = 4$ and further investigate the geometry by analyzing the Euclidean action and the corresponding partition function. Higher-dimensional cases will also be briefly discussed. Finally, as the last discussion in this section, let us examine the limit $m \rightarrow 0$. In this case, the solution (2.25) behaves asymptotically as

$$\begin{aligned} N(r) &= \frac{-8\pi\lambda m^2}{d} \sqrt{1 - \frac{m^{d-1}}{r^{d-1}}} \int_{m/r_c}^{m/r} \frac{1}{x^3 (1-x^{d-1})^{3/2}} dx \\ &= \frac{-8\pi\lambda m^2}{d} \int_{m/r_c}^{m/r} \frac{1}{x^3} + \mathcal{O}\left(\frac{1}{x^2}\right) dx \\ &= \frac{4\pi\lambda}{d} (r^2 - r_c^2) + \mathcal{O}(m). \end{aligned} \quad (2.27)$$

Accordingly, the finite spatial volume takes the form

$$\begin{aligned} V &= \Omega_d m^{d+1} \int_{m/r_c}^1 \frac{1}{(1-x^{d-1})^{1/2} x^{d+2}} dx \\ &= \Omega_d m^{d+1} \int_{m/r_c}^1 \frac{1}{x^{d+2}} + \mathcal{O}\left(\frac{1}{x^{d+3}}\right) dx \\ &= \frac{\Omega_d}{d+1} r_c^{d+1} + \mathcal{O}(m). \end{aligned} \quad (2.28)$$

Naturally, the leading-order behavior of the solution in this limit reproduces Eq. (2.3), while the higher-order corrections originate from the nonvanishing mass parameter.

For convenience, we refer to the solutions of Einstein gravity subject to a fixed-volume constraint as volume-constrained Euclidean geometries (VCEGs). The configuration with a vanishing mass constant ($M = 0$) will be referred to as the massless VCEG, whereas those with a nonzero mass constant ($M \neq 0$) will be termed massive VCEG.

3 Euclidean formalism and Iyer-Wald entropy

In the previous section, we discussed the gravitational solution associated with a nonzero constant mass function. As shown in Eq. (2.25), the expression for $N(r)$ is rather complicated, which may lead to difficulties in evaluating the Euclidean action. To better and more transparently identify the contribution of the geometry to the Euclidean action (2.1), we now turn to a more general discussion based on the covariant phase space formalism.

In the context of gravitational theories, general covariance constitutes the fundamental gauge symmetry. Within the covariant phase space formalism, such symmetries give rise to conserved surface charges associated with exact spacetime symmetries. These charges provide a direct derivation of the first law of black hole thermodynamics [30, 41], and furthermore, naturally encode the relation between Noether charges and the on-shell gravitational action [20, 30, 42]. When a volume constraint is imposed in the action, however, subtleties arise in the covariant phase space construction: since the spatial volume of each spacelike slice is fixed, the original diffeomorphism invariance is partially broken. Nevertheless, the relation between Noether charges and the on-shell gravitational action can still be established. Related discussions can be found in the Supplemental Material of Ref. [27]. Here we provide a parallel review, together with explicit derivations and a more detailed discussion.

To begin with, the bulk part of the Euclidean action (2.1) for D -dimensional gravitational theories at finite volume can be expressed as

$$I_{\text{bulk}} = - \int \mathbf{L}, \quad (3.1)$$

where

$$\mathbf{L} = \mathbf{L}_G + \lambda(\tau) d\tau \wedge (\sqrt{\gamma} (d^{D-1}x)_\tau - v \sqrt{\gamma} (d^{D-1}x)_\tau), \quad (3.2)$$

$$v = V \left(\int_{\partial\Sigma_\tau} \sqrt{\gamma} (d^{D-1}x)_\tau \right)^{-1}. \quad (3.3)$$

Here, \mathbf{L}_G represents the purely gravitational part, which we assume to be generally covariant. In the case of Einstein gravity, it is given by

$$\mathbf{L}_G = \frac{1}{16\pi} \sqrt{g} R d^D x. \quad (3.4)$$

To express the action in the form of a D -form, the nonlocal term v is introduced. However, the second term in Eq. (3.2) does not constitute a strictly proper D -form. This reflects an explicit

breaking of the full diffeomorphism invariance of the bulk manifold M , reducing the symmetry effectively to independent diffeomorphisms acting on the Euclidean time circle \mathbb{S}^1 and on the spatial slice Σ_τ . Consequently, directly applying the covariant phase-space formalism to the full Lagrangian density (3.2) involves certain technical complications. Nonetheless, it should be emphasized that our primary objective is to establish the relationship between the Noether charge and the geometric contributions to the Euclidean action. Since all geometries under consideration satisfy the volume constraint, only the purely gravitational term \mathbf{L}_G gives a nonvanishing contribution to the Euclidean bulk action I_E . Therefore, it suffices to apply the covariant phase-space method to the generally covariant gravitational part \mathbf{L}_G alone.

By varying the Lagrangian density \mathbf{L}_G with respect to g_{ab} , one finds

$$\delta \mathbf{L}_G = \mathbf{E}[g]^{ab} \delta g_{ab} + d\Theta[g, \delta g], \quad (3.5)$$

where $\mathbf{E}[g]^{ab}$ denotes the Euler-Lagrange expression for the gravitational sector, and $\Theta[g, \delta g]$ is the associated presymplectic potential. In the case of Einstein gravity, these are explicitly given by

$$\mathbf{E}[g]^{ab} = E[g]^{ab} \sqrt{g} d^D x = \frac{1}{16\pi} \left(\frac{1}{2} g^{ab} R - R^{ab} \right) \sqrt{g} d^D x, \quad (3.6)$$

$$\Theta[g, \delta g] = \frac{1}{16\pi} \sqrt{g} \left(g^{ca} \nabla^b - g^{ab} \nabla^c \right) \delta g_{ab} (d^{D-1} x)_c. \quad (3.7)$$

Next, consider the field transformation generated by a vector field ξ^a , under which the metric varies as

$$\delta_\xi g_{ab} \equiv \mathcal{L}_\xi g_{ab} = \nabla_a \xi_b + \nabla_b \xi_a, \quad (3.8)$$

corresponding to an infinitesimal diffeomorphism. Under this transformation, one finds,

$$\delta_\xi \mathbf{L}_G = \mathcal{L}_\xi \mathbf{L}_G = d(i_\xi \mathbf{L}_G). \quad (3.9)$$

On the other hand, applying (3.5) gives

$$\delta_\xi \mathbf{L}_G = 2\mathbf{E}[g]^{ab} \nabla_a \xi_b + d\Theta[g, \delta_\xi g], \quad (3.10)$$

Hence, we obtain

$$d(i_\xi \mathbf{L}_G) = 2\mathbf{E}[g]^{ab} \nabla_a \xi_b + d\Theta[g, \delta_\xi g]. \quad (3.11)$$

Taking the Euler-Lagrange derivative (see, e.g., [48, 49] for related definitions) with respect to ξ_a on both sides, the exact form terms drop out, leaving

$$\nabla_a E[g]^{ab} = 0. \quad (3.12)$$

This, in turn, implies that Eq. (3.11) can be rewritten as

$$d(i_\xi \mathbf{L}_G - \mathbf{M}[\xi] - \Theta[g, \delta_\xi g]) = 0, \quad (3.13)$$

where

$$\mathbf{M}[\xi] = 2\xi_a E[g]^{ab} (\mathrm{d}^{D-1}x)_b. \quad (3.14)$$

By the algebraic Poincaré lemma [48, 49], locally there exists a Noether charge $\mathbf{Q}[\xi]$ such that

$$i_\xi \mathbf{L}_G - \mathbf{M}[\xi] - \Theta[g, \delta_\xi g] = -\mathrm{d}\mathbf{Q}[\xi]. \quad (3.15)$$

It should be noted that the Noether charge $\mathbf{Q}[\xi]$ is not uniquely defined; in what follows, we adopt the Noether-Wald Norther charge [41]. A direct computation shows that the Noether charge for Einstein gravity is

$$\mathbf{Q}[\xi] \equiv -\frac{1}{8\pi} \sqrt{g} \nabla^a \xi^b (\mathrm{d}^d x)_{ab}. \quad (3.16)$$

Substituting this into Eq. (3.15) with $\xi = \partial_\tau$ and integrating over Σ_τ , one finds

$$-\int_{\Sigma_\tau} i_{\partial_\tau} \mathbf{L}_G = \int_{\partial\Sigma_\tau} \mathbf{Q}[\partial_\tau] - \int_{\Sigma_\tau} \Theta[g, \delta_{\partial_\tau} g] - \int_{\Sigma_\tau} \mathbf{M}[\partial_\tau]. \quad (3.17)$$

Inspecting Eq. (3.14) shows that the third term is tied to the $\tau\tau$ - and τi -components of the gravitational field equations, namely, the Hamiltonian and momentum constraints. As Eq. (2.2) makes clear, the volume constraint leaves these constraints unchanged. Hence, provided the Hamiltonian and momentum constraints are satisfied, even with the volume constraint imposed, the third term contributes nothing. If the Euclidean geometry further admits translational symmetry along the τ -direction, the second term also vanishes. Under these considerations, the bulk gravitational action reduces to the boundary contribution $\mathbf{Q}[\partial_\tau]$ at ∂M . Performing the remaining integration over the τ -direction, for Euclidean geometries that satisfy the volume constraint, we obtain

$$I_{\text{bulk}} = -\int_M \mathbf{L} = -\int_0^\beta d\tau \int_{\Sigma_\tau} i_{\partial_\tau} \mathbf{L}_G = \int_0^\beta d\tau \int_{\partial\Sigma_\tau} \mathbf{Q}[\partial_\tau]. \quad (3.18)$$

If $\partial\Sigma_\tau$ includes the bifurcation surface \mathcal{B} (i.e., Σ_τ intersects the Killing horizon associated with ∂_τ), then the boundary term in Eq. (3.18) evaluated on \mathcal{B} yields the Wald entropy S_W , which in general relativity reduces to one quarter of the horizon area.

In the Euclidean action (2.1), the Gibbons-Hawking-York term contributes only when the manifold M has a boundary; if M is boundaryless, the action is entirely determined by the bulk term. In this case, the Euclidean action reduces to a surface integral over $\partial\Sigma_\tau$, and when $\partial\Sigma_\tau = \mathcal{B}$, it is fixed solely by the horizon contribution S_W . For Einstein gravity, three-dimensional massive gravity, and Lovelock gravity, it has been shown [27–29] that the on-shell Euclidean action coincides with the Wald entropy, giving the semiclassical partition function $\mathcal{Z} \sim e^{S_W}$.

In the subsequent analysis of the Euclidean action, Eq. (3.18) greatly simplifies the computation. In particular, as shown in Eq. (2.25), the integral defining $N(r)$ is intrinsically complicated, making the evaluation of the bulk contribution for the metric (2.22) rather difficult. Equation (3.18), however, shows that it is sufficient to consider only the metric at $\partial\Sigma_\tau$.

4 Geometric contributions to the Euclidean action

In Sec. 2, we examined spherically symmetric geometries in dimensions $d \geq 4$, characterized by $p(r) = \lambda/N(r)$. For the solutions to satisfy the field equations, the condition (2.11) must hold. Two distinct cases were considered, namely $p'(r) = 0$ and $\rho(r) = 0$. In both situations, compact geometries emerge only when $\lambda < 0$; otherwise, the spatial volume diverges. In the first case, the energy density is nonvanishing and uniformly distributed throughout spacetime, leading to the geometry $\mathbb{S}^1 \times \mathbb{S}^{d+1}$. However, this configuration does not correspond to a genuine gravitational solution of the action in Eq. (2.1). By contrast, in the second case, the energy density vanishes while the mass function $M(r)$ may remain nonzero. The resulting geometry constitutes a genuine gravitational solution of Eq. (2.1), thereby extending the class of configurations originally considered in Ref. [27]. In what follows, we focus on the solution discussed in Sec. 2.2 and evaluate its contribution to the Euclidean action I_E (2.1).

4.1 General considerations

Before evaluating the contribution of the on-shell solution to the Euclidean action, let us first consider a more general class of Euclidean geometries,

$$ds^2 = N(r)^2 d\tau^2 + \left(1 - \frac{m^{d-1}}{r^{d-1}}\right)^{-1} dr^2 + r^2 d\Omega_d^2, \quad (4.1)$$

which corresponds to the metric ansatz (2.6) satisfying Eq. (2.7). These geometries represent gravitational metric that satisfy both the Hamiltonian and momentum constraints. Consequently, for the full Euclidean action (2.1), the bulk contribution can be expressed in terms of $\mathbf{Q}[\partial_\tau]$ evaluated on the boundaries of Σ_τ at $r = r_c$ and $r = m$, while the Gibbons-Hawking-York term is added at the manifold boundary $r = m$. For the bulk contribution, one finds

$$I_{\text{bulk}} = \beta_H Q_S(r_c) - \beta_H Q_S(m), \quad (4.2)$$

where

$$Q_S(r) = \frac{1}{8\pi} \left(1 - \frac{m^{d-1}}{r^{d-1}}\right)^{1/2} N'(r) \Omega_d r^d, \quad (4.3)$$

$$\beta_H = -2\pi \left(1 - \frac{m^{d-1}}{r_c^{d-1}}\right)^{-1/2} \frac{1}{N'(r_c)}. \quad (4.4)$$

Here, β_H denotes the period of the Euclidean time coordinate τ required to eliminate the conical singularity, corresponding to the inverse temperature. The Gibbons-Hawking-York term contributes at the boundary $r = m$, yielding

$$\begin{aligned} & -\frac{1}{8\pi} \int_{r=m} \sqrt{h} K d^{d+1}x \\ &= \frac{\beta_H d}{8\pi} \left(1 - \frac{m^{d-1}}{r^{d-1}}\right)^{1/2} N(r) \Omega_d r^{d-1} \Big|_{r=m} + \frac{\beta_H}{8\pi} \left(1 - \frac{m^{d-1}}{r^{d-1}}\right)^{1/2} N'(r) \Omega_d r^d \Big|_{r=m}. \end{aligned} \quad (4.5)$$

The full Euclidean action thus receives contributions from both $r = m$ and $r = r_c$. At $r = m$, one finds

$$-\beta_H Q_S(m) - \frac{1}{8\pi} \int_{r=m} \sqrt{h} K d^{d+1}x = \frac{\beta_H d}{8\pi} \left(1 - \frac{m^{d-1}}{r^{d-1}}\right)^{1/2} N(r) \Omega_d r^{d-1} \Big|_{r=m}, \quad (4.6)$$

This contribution vanishes whenever $N(m)$ is finite, which is indeed the case for the solution $N(r)$ given by Eq. (2.25). At $r = r_c$, one instead obtains

$$\beta_H Q_S(r_c) = -\frac{1}{4} \Omega_d r_c^d. \quad (4.7)$$

Therefore, for the metric (4.1), the total contribution to the Euclidean action (2.1) is

$$I_E = -\frac{1}{4} \Omega_d r_c^d = -\frac{1}{4} \mathcal{A}_c, \quad (4.8)$$

where \mathcal{A}_c denotes the horizon area at $r = r_c$. Remarkably, despite the presence of the mass parameter m , the Euclidean action of the massive VCEG continues to reproduce the standard area law, identical to that of the massless VCEG [27]. Compared with the original result for the massless VCEG, a positive mass parameter m gives rise to a massive VCEG possessing a geometric boundary with topology $\mathbb{S}^1 \times \mathbb{S}^d$, which contributes a vanishing term to the action.

It is worth noting that, in contrast to the massless VCEG, massive VCEG possesses a boundary at $r = m$. From the viewpoint of the Euclidean action (or equivalently the free energy $F = I_E/\beta_H$), one finds that the total energy of VCEG vanishes, even though the parameter m is nonzero. On the other hand, the gravitational energy should be defined by the Arnowitt-Deser-Misner (ADM) Hamiltonian H_{ADM} associated with ∂_τ , which is determined by the boundary at $r = m$,

$$H_{\text{ADM}} = -\frac{1}{8\pi} \int_{r=m} N \mathcal{K} r^d d\Omega_d = \frac{d}{8\pi} \left(1 - \frac{m^{d-1}}{r^{d-1}}\right)^{1/2} N(r) \Omega_d r^{d-1} \Big|_{r=m}, \quad (4.9)$$

where \mathcal{K} denotes the trace of extrinsic curvature of the hypersurface $r = m$ within the time slice $\Sigma\tau$. Clearly, this contribution vanishes, and moreover it coincides with Eq. (4.6) up to an overall factor of β_H . This again confirms that the Euclidean action is governed by the area law. Therefore, unlike in the Schwarzschild black hole, the parameter m here does not represent a gravitational energy. Up to this point, it may seem that the parameter m has no effect on the Euclidean action. However, this is not the case. When the metric is taken on-shell, an additional volume constraint equation (2.26) must be satisfied. This relation implies that different values of m correspond to different values of r_c , so that r_c can be regarded as a function of m . Consequently, the Euclidean action is indirectly determined by m .

So far, our discussion has been fairly general. To make the analysis more concrete, we now focus on the four-dimensional case ($D = 4$, $d = 2$).

4.2 The four-dimensional case

Let us now turn to the case of $D = 4$ ($d = 2$), where the structure of VCEG becomes more transparent. In this setting, once the rr -component of the field equations is imposed, the metric function $N(r)$ in Eq. (4.1) is determined explicitly by Eq. (2.25), yielding

$$\begin{aligned} N(r) = & \pi \lambda r^2 \left(2 + \frac{5m}{r} - \frac{15m^2}{r^2} \right) \\ & + \pi \lambda \sqrt{1 - \frac{m}{r}} \left(\frac{1}{\sqrt{1 - m/r_c}} (15m^2 - 5r_c m - 2r_c^2) - 15m^2 \operatorname{arctanh} \left(\sqrt{1 - \frac{m}{r_c}} \right) \right) \\ & + 15\pi \lambda m^2 \sqrt{1 - \frac{m}{r}} \operatorname{arctanh} \left(\sqrt{1 - \frac{m}{r}} \right). \end{aligned} \quad (4.10)$$

It is straightforward to verify that $N(r)$ remains strictly non-negative in the range $m \leq r \leq r_c$, with boundary values $N(m) = -8\pi \lambda m^2 \geq 0$ and $N(r_c) = 0$. The elimination of the conical singularity at $r = r_c$ requires a specific periodicity of the Euclidean time coordinate. Consequently, the associated Hawking temperature (or inverse temperature) is determined by

$$T_c = \frac{1}{\beta_c} = -2\lambda r_c \left(1 - \frac{m}{r_c} \right)^{-1/2}, \text{ or } \beta_c = -\frac{1}{2\lambda r_c} \sqrt{1 - \frac{m}{r_c}}. \quad (4.11)$$

As the lapse function, $N(r)$ depends on the parameters λ , m , and r_c . The constant λ can be absorbed into a rescaling of the Euclidean time coordinate τ , accompanied by a redefinition of its period β_c . By contrast, the parameters m and r_c are correlated through the volume constraint. Specifically, for $d = 2$, the constrained spatial volume, as given by Eq. (2.26), takes the form

$$V = \frac{4}{3} \pi r_c^3 \left(\sqrt{1 - \frac{m}{r_c}} \left(1 + \frac{5m}{4r_c} + \frac{15m^2}{8r_c^2} \right) + \frac{15m^3}{8r_c^3} \operatorname{arctanh} \left(\sqrt{1 - \frac{m}{r_c}} \right) \right). \quad (4.12)$$

Thus, the geometry of the metric is effectively determined by a single parameter, the mass parameter m . Representative profiles of $N(r)$ for different values of m are displayed in Fig. 1. As the figure illustrates, m not only sets the lower cutoff at $r = m$ but also determines the upper bound r_c . To make the functional dependence between m and r_c more transparent, we further plot the implicit relation obtained from Eq. (4.12) for a fixed volume $V = 4\pi/3$, as shown in Fig. 2. The plot reveals two salient features. First, the relation between r_c and m is initially monotonic decreasing, reaches a minimum, and then turns into a monotonic increasing branch. Second, for large values of m , the blue curve asymptotically approaches the red dashed line $r_c = m$, indicating that $m/r_c \rightarrow 1^-$. In this regime, the radial domain (m, r_c) of VCEG becomes increasingly narrow. Consistently, evaluating the proper radial distance,

$$\int_m^{r_c} \left(1 - \frac{m}{r} \right)^{-1/2} dr, \quad (4.13)$$

shows that it decreases with growing m . The same behavior can be inferred from the volume expression (2.26): as both m and r_c increase, the spherical part of the volume element grows, and under the constraint of fixed total volume, the proper radial extension must shrink accordingly. Thus, the spatial geometry asymptotically approaches that of a thin spherical shell.

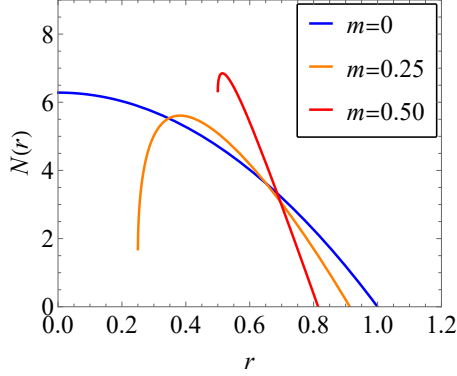


Figure 1. Functional profiles of $N(r)$ at fixed volume $V = 4\pi/3$. The blue, orange, and red curves correspond to $m = 0$ ($r_c = 1$), $m = 0.25$ ($r_c \approx 0.91$), and $m = 0.5$ ($r_c \approx 0.81$), respectively. Throughout the plot, the parameter λ is fixed at -1 .

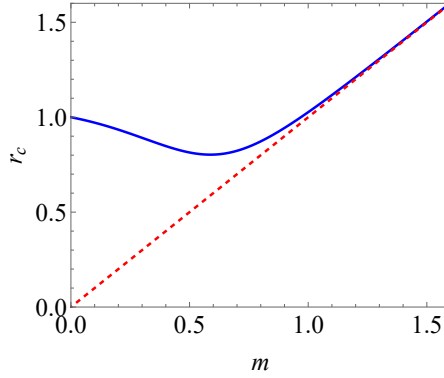


Figure 2. Relation between the mass parameter m and r_c at fixed volume. The volume is chosen to be that of a unit ball in three dimensions, $V = 4\pi/3$. The blue curve represents the functional dependence of m on r_c , while the red dashed line corresponds to $r_c = m$.

We now turn to the contribution of this geometry to the Euclidean action. From Eq. (4.8), one immediately obtains

$$I_E = -\pi r_c^2. \quad (4.14)$$

Taking into account the volume constraint (4.12), the Euclidean action is therefore effectively a function of the mass parameter m . The corresponding functional relation between m and I_E is displayed in Fig. 3. On the other hand, the partition function is related to the Euclidean

action via

$$\mathcal{Z} = \exp(-I_E) = \exp(\pi r_c^2). \quad (4.15)$$

It is evident that near $m = 0$, introducing the cutoff at $r = m$ leads to an increase in I_E , thereby suppressing the partition function. In contrast, for large m , the cutoff also raises I_E , but in this case it enhances the partition function. From a geometric perspective, for large values of the mass parameter m , the radius r_c grows accordingly. To preserve the fixed volume, the geometry effectively becomes a thin spherical shell, whose partition function is determined entirely by its surface area.

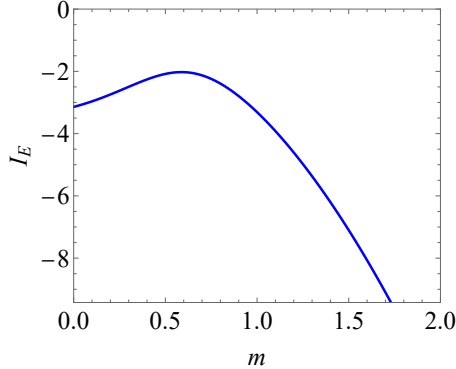


Figure 3. Relation between the mass parameter m and the Euclidean action I_E at fixed volume $V = 4\pi/3$.

5 Extension of the volume-constrained Euclidean geometry

In the preceding section, we analyzed a class of Euclidean geometries, the massive volume-constrained Euclidean solutions, which emerge when the mass parameter m (or mass constant M) is nonzero. Compared to massless VCEGs, a nonzero m introduces a cutoff of spacetime at a finite radius. As shown in the metric (2.22), the region $r < m$ is unphysical, suggesting that one must introduce a cutoff surface at $r = m$ to serve as the spacetime boundary. At this surface, the boundary geometry takes the form of a direct product $\mathbb{S}^1 \times \mathbb{S}^d$, with respective radii $N(m)$ and m , forming a finite throat. This indicates that the spacetime does not genuinely end at $r = m$; instead, the boundary at $r = m$ is merely an artificial construct. Furthermore, as shown in Fig. 1, the derivative of $N(r)$ diverges at $r = m$, signaling that r is not a suitable coordinate near this region. These observations point to the need for an alternative coordinate system that renders the metric (2.22) better behaved and allows for a smooth extension.

To achieve this, we introduce the coordinate,

$$\cos^2 \chi = \frac{m^{d-1}}{r^{d-1}}, \quad \text{or equivalently} \quad \chi = \arccos \left((m/r)^{(d-1)/2} \right). \quad (5.1)$$

The range $r \in [m, r_c]$ is then mapped to $\chi \in [0, \chi_c]$, where

$$\chi_c = \arccos \left((m/r_c)^{(d-1)/2} \right), \quad (5.2)$$

establishing a one-to-one correspondence between the two variables. In terms of coordinate χ , the metric

$$ds^2 = N(\chi)^2 d\tau^2 + \frac{4m^2}{(d-1)^2} \cos(\chi)^{-2(d+1)/(d-1)} d\chi^2 + r(\chi)^2 d\Omega_d^2, \quad (5.3)$$

with lapse function $N(\chi) \equiv N(r(\chi))$, despite the slight abuse of notation. Importantly, the coordinate transformation is technically degenerate at $r = m$, since $\partial_\chi r(\chi)|_{\chi=0} = 0$. However, this very feature eliminates the divergence that was present in the radial component of the metric. Moreover, in the new coordinate χ , the factor $\sqrt{1 - m^{d-1}/r^{d-1}}$ in the lapse function $N(r)$ is replaced by $\sin \chi$, thereby avoiding coordinate singularities. For instance, in four dimensions, the derivative of $N(r)$ with respect to r diverges, as illustrated in Fig. 1. By contrast, in terms of χ , the function $N(\chi)$ is analytic. We demonstrate this explicitly in the cases of $D = 4$ and higher dimensions.

Since the range of r is $[m, r_c]$ with $r = m$ as a boundary, the corresponding range of χ is $[0, \chi_c]$ with $\chi = 0$ serving as a boundary. In the original metric (2.22), the restriction $r \geq m$ ensures that no unphysical region with two time directions arises in the Lorentzian continuation, and $r < m$ is regarded as inaccessible. By contrast, in the metric (5.3), the coordinate χ can smoothly pass through the boundary at $\chi = 0$, which is a direct consequence of the transformation in Eq. (5.1). This indicates that the original geometry for $\chi \in [0, \chi_c]$ can be extended to $\chi \in [\chi_e, \chi_c]$, with $\chi_e \in [-\pi/2, 0]$ defined by the condition $N(\chi_e) = 0$. The extended geometry no longer possesses a truncated boundary and features two horizons located at $\chi = \chi_e$ and $\chi = \chi_c$, closely resembling the structure of SdS black hole. We refer to this extended configuration as the extended VCEG. Moreover, examining the line element in Eq. (5.3), one can naturally interpret r as the radius of the spherical section of the metric. At $\chi = 0$, the radius $r(\chi)$ reaches its minimum value, indicating that $\chi = 0$ (or equivalently $r = m$) corresponds to a wormhole-like throat.

5.1 The four-dimensional case

We now turn to the four-dimensional case. In Sec. 4.2, we discussed the VCEG, where the spacetime terminates at the boundary $r = m$. Although this boundary is present, it does not contribute to the energy, and the Euclidean action receives contributions solely from the horizon area at $r = r_c$. However, in the limit of large m , despite the finiteness of the spatial volume, the free energy is unbounded from below and diverges to negative infinity. Let us now consider the four-dimensional extended VCEG. Starting from the lapse function $N(r)$ in Eq. (4.10), and performing the coordinate transformation $\cos^2 \chi = m/r$, we obtain

$$N(\chi) = -\pi \lambda m^2 \sin \chi \left(-15 \operatorname{arctanh}(\sin \chi) + \frac{15 \cos^4 \chi - 5 \cos^2 \chi - 2}{\sin \chi \cos^4 \chi} + 15 \operatorname{arctanh}(\sin \chi_c) - \frac{15 \cos^4 \chi_c - 5 \cos^2 \chi_c - 2}{\sin \chi_c \cos^4 \chi_c} \right), \quad (5.4)$$

where $\chi_c = \arccos(\sqrt{m/r_c})$ denotes the largest zero of $N(\chi)$. The behavior of $N(\chi)$ is illustrated in Fig. 4. We observe that $N(\chi)$ generally possesses two zeros: the positive one

at χ_c and another negative one at χ_e . Moreover, $N(\chi)$ is not generically symmetric under $\chi \rightarrow -\chi$. This structure can be seen in Eq. (5.4), where the first line of the bracketed expression is odd in χ , while the second line is an even (constant) term. Only when the constant term vanishes does $N(\chi)$ become symmetric. In this case, the corresponding root is denoted as χ_c^* , with the second root located at $\chi_e = -\chi_c^*$. Numerically, we obtain $\chi_c^* \approx 0.54$. Moreover, Eq. (5.4) implies that once χ_c is fixed, χ_e is determined uniquely; their relation is plotted in Fig. 5(a). A close inspection shows that the relation between χ_e and χ_c is nonlinear. In particular, as $\chi_c \rightarrow 0$ one finds $\chi_e \rightarrow -\pi/2$, so the extended coordinate range approaches $(-\pi/2, 0)$. Conversely, as $\chi_c \rightarrow \pi/2$ one has $\chi_e \rightarrow 0$, and the range approaches $(0, \pi/2)$.

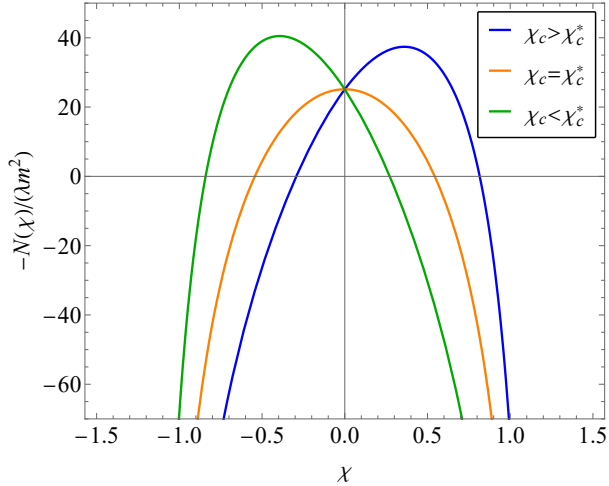


Figure 4. Profile of the lapse function $N(\chi)$. The curves with different colors correspond to different parameter choices: the blue curve represents the case $\chi_c > \chi_c^*$, the orange curve corresponds to $\chi_c = \chi_c^*$, and the green curve denotes $\chi_c < \chi_c^*$. The critical value χ_c^* is defined by the condition $H(\chi_c^*) = 0$.

From a geometric perspective, the extended solution is compact and contains no boundary. In this case, the geometry admits a Euclidean time direction, and since $N(\chi_e) = N(\chi_c) = 0$ at both $\chi = \chi_e$ and $\chi = \chi_c$, the spacetime features two horizons. To avoid conical singularities, each horizon imposes a periodicity on the Euclidean time coordinate, yielding the corresponding inverse temperatures

$$\beta_c = \frac{-4\pi m}{N'(\chi_c) \cos^3 \chi_c}, \quad \beta_e = \frac{4\pi m}{N'(\chi_e) \cos^3 \chi_e}, \quad (5.5)$$

respectively. In general, these two periods are unequal, except when $\chi_c = \chi_c^*$, which indicates that the geometry typically contains at least one conical singularity. Along the radial direction, each value of r defines a spherical section \mathbb{S}^2 , with the radius attaining its minimum $r = m$ at $\chi = 0$, thereby forming a throat reminiscent of a wormhole. Altogether, this geometry resembles that of a Euclidean dS black hole, while simultaneously exhibiting wormhole-like features, bounded between the two horizons. A schematic illustration is shown in Fig. 6.

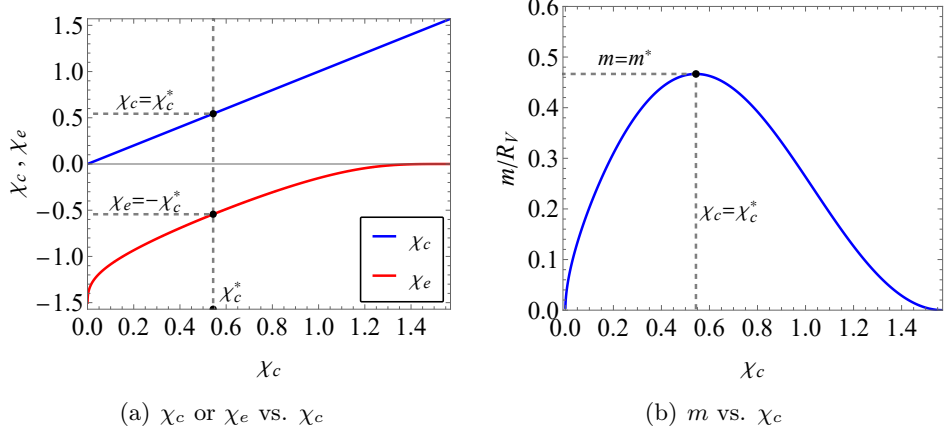


Figure 5. Relations among the characteristic parameters of the metric, m , χ_e , and χ_c . (a) The dependence of χ_c and χ_e on χ_c . The blue and red curves correspond to χ_c and χ_e , respectively, where χ_c and χ_e denote the two roots of the lapse function $N(\chi)$. (b) The relation between the mass parameter m and χ_c . The mass parameter reaches its maximal value m^* when $\chi_c = \chi_c^*$.

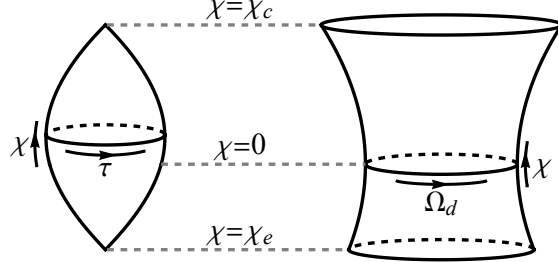


Figure 6. Schematic illustration of the extended VCEG. The left panel shows the Euclidean section in the (τ, χ) plane, forming a double-cone structure with tips at $\chi = \chi_e$ and $\chi = \chi_c$, which define the allowed range $\chi_e < \chi < \chi_c$. The right panel depicts the (χ, Ω_d) section, where the spherical radius reaches its minimum at $\chi = 0$, corresponding to the throat of the geometry with radius equal to the mass parameter m . The maximum of the lapse function $N(\chi)$ lies above the throat, as illustrated here for $\chi_c > \chi_c^*$. For $\chi_c = \chi_c^*$ or $\chi_c < \chi_c^*$, the extremum coincides with or lies below the throat, respectively.

In addition to the equations of motion, there exists a further constraint, namely the volume constraint,

$$V = \frac{\pi}{6} m^3 \left(15 \operatorname{arctanh}(\sin \chi_c) + \frac{\sin \chi_c}{\cos^6 \chi_c} (15 \cos^4 \chi_c + 10 \cos^2 \chi_c + 8) - 15 \operatorname{arctanh}(\sin \chi_e) - \frac{\sin \chi_e}{\cos^6 \chi_e} (15 \cos^4 \chi_e + 10 \cos^2 \chi_e + 8) \right). \quad (5.6)$$

The volume constraint relates m , χ_e , and χ_c . Since χ_e is determined by χ_c , it follows that m

is also fixed once χ_c is specified, as illustrated in Fig. 5(b). Furthermore, from the periodicity of τ given in Eq. (5.5), one sees that λ , appearing as the overall coefficient of $N(r)$, can be used to adjust the relation between the conical deficit and the Euclidean time period, and can effectively be absorbed into the coordinate τ . Consequently, the extended VCEG in this case is essentially determined by the single parameter χ_c .

On the other hand, viewed in reverse, when the mass parameter m is specified, the values of χ_e and χ_c can be obtained by solving Eq. (5.6) together with the condition $N(\chi_e) = 0$. A noteworthy feature of these solutions is the presence of an underlying \mathbb{Z}_2 symmetry: if $(\chi_c, \chi_e) = (\hat{\chi}_c, \hat{\chi}_e)$ is a solution, then $(\chi_c, \chi_e) = (-\hat{\chi}_e, -\hat{\chi}_c)$ is also a solution. Moreover, one finds

$$N(\chi)|_{\chi_c=\hat{\chi}_c} = N(-\chi)|_{\chi_c=-\hat{\chi}_e}, \quad (5.7)$$

and since the rr - and angular components of the metric in the present coordinate system are even functions of χ , we conclude that the two cases $\chi_c = \hat{\chi}_c$ and $\chi_c = -\hat{\chi}_e$ are in fact degenerate. They correspond to the same geometry, related by the coordinate transformation $\chi \rightarrow -\chi$. As a consequence, the effective range of χ_c is restricted to $[0, \chi_c^*]$ or $[\chi_c^*, \pi/2]$, where χ_c^* is indicated in Fig. 5(a). Alternatively, the geometry can be parametrized by m , whose range is $[0, m^*]$, with m^* marked in Fig. 5(b). Nevertheless, for practical convenience, we shall often use χ_c to characterize the geometry, despite the possible degeneracy.

One point deserves attention. When m vanishes identically (equivalently $\chi_c = 0$ or $\chi_c = \pi/2$), the metric degenerates in the corresponding components and thus becomes ill-defined. However, an asymptotic analysis shows that as $\chi_c \rightarrow \pi/2$ one has $m \rightarrow 0$ and $\chi_e \rightarrow 0$. Using the coordinate transformation (5.1), the resulting geometry approaches the massless VCEG (2.3) (after an appropriate choice of λ the two metrics coincide). This indicates that the extended massless VCEG coincides with the massless VCEG itself; in other words, when the mass parameter vanishes, no further extension is required.

We now turn to the contribution of the Euclidean geometry to the action. As discussed in Sec. 3, the action receives contributions only from the horizon terms. In contrast to the previous case, however, here conical singularities are present, and one must add the corresponding contributions from $\chi = \chi_c$ and $\chi = \chi_e$. For Einstein gravity these take the form [20, 40, 50–53]

$$-\frac{1}{4}\mathcal{A}_c\left(1 - \frac{\beta}{\beta_c}\right) - \frac{1}{4}\mathcal{A}_e\left(1 - \frac{\beta}{\beta_e}\right), \quad (5.8)$$

where \mathcal{A}_c and \mathcal{A}_e denote the horizon areas at χ_c and χ_e , respectively. The resulting Euclidean action is then

$$I_E = -\frac{1}{4}(\mathcal{A}_c + \mathcal{A}_e) = -\left(\frac{\pi m^2}{\cos^4 \chi_c} + \frac{\pi m^2}{\cos^4 \chi_e}\right). \quad (5.9)$$

This expression depends solely on the horizon areas. Furthermore, the result is independent of λ , indicating that I_E is a function only of χ_c (or, equivalently, of m). The corresponding curves are shown in Fig. 7(a) and Fig. 7(b), with the ball volume given by $V = 4\pi R_V^3/3$. One observes that the Euclidean action is bounded from below, with the lower bound $I_E = -\pi R_V^2$

attained in the limit $\chi_c = 0$ or $\chi_c = \pi$ (equivalently $m = 0$). This indicates that excitations of the mass constant increase the Euclidean action or the free energy.

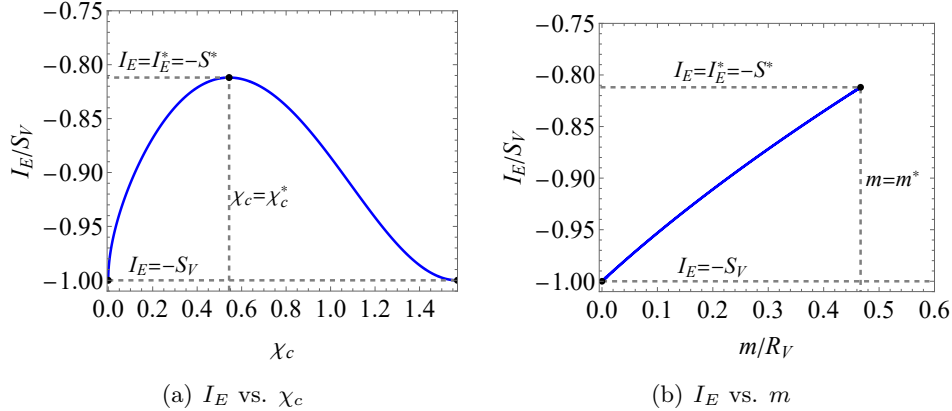


Figure 7. Euclidean action as a function of m and χ_c . The curves marked with an asterisk correspond to the critical configuration with $\chi_c = \chi_c^*$ and $m = m^*$.

5.2 Higher-dimensional extension

For dimensions higher than four, a similar analysis can be carried out. However, under the volume constraint, the solutions, VCEG, become significantly more complicated, as illustrated in Eq. (2.25). Nevertheless, many qualitative properties of the solutions can still be inferred directly from the equations of motion. In terms of the coordinate transformation (5.1), Eq. (2.23) (or equivalently the field equations) yields the differential equation for $N(\chi)$,

$$N'(\chi) = \frac{d(d-1) \cos \chi N(\chi) + 16\pi\lambda m^2 \cos(\chi)^{-(d+3)/(d-1)}}{d(d-1) \sin \chi}. \quad (5.10)$$

As in the analysis of $N(r)$, finiteness of the spatial volume requires $\lambda < 0$. Near the endpoints $\chi \rightarrow \pm\pi/2$, one finds the asymptotic behavior

$$N(\chi) \sim \lambda (\cos \chi)^{-4/(d-1)}. \quad (5.11)$$

Since the valid region of the geometry is defined by the condition $N(\chi) > 0$, the function $N(\chi)$ must necessarily possess at least two zeros. At such zeros, say at χ_0 where $N(\chi_0) = 0$, Eq. (5.10) reduces to

$$N'(\chi_0) = \frac{16\pi\lambda m^2}{d(d-1) \sin \chi_0} \cos(\chi_0)^{-(d+3)/(d-1)}. \quad (5.12)$$

This expression shows that the sign of $N'(\chi_0)$ at a zero is fixed: for a zero located at $\chi_0 > 0$, one has $N'(\chi_0) < 0$, while for a zero located at $\chi_0 < 0$, one has $N'(\chi_0) > 0$. Consequently, the metric function $N(\chi)$ generally possesses exactly one positive root and one negative root.

In analogy with the four-dimensional case, we denote the positive root by χ_c and the negative one by χ_e . For the differential equation (5.10) with the boundary condition $N(\chi_c) = 0$, we can obtain the lapse function as,

$$\begin{aligned} N(\chi) &= -\frac{16\pi\lambda m^2}{d(d-1)} \sin \chi (H(\chi) - H(\chi_c)), \\ H(\chi) &= \frac{\cos \chi}{\sin \chi} {}_2F_1\left(-\frac{1}{2}, -\frac{d+3}{2(d-1)}; \frac{1}{2}; -\tan^2 \chi\right), \end{aligned} \quad (5.13)$$

where ${}_2F_1$ denotes the Gauss hypergeometric function. Meanwhile, the volume constraint yields

$$V = \frac{2m^d \Omega_d}{d-1} \left({}_2F_1\left(\frac{1}{2}, \frac{2d}{d-1}; \frac{3}{2}; \sin^2 \chi_c\right) \sin \chi_c - {}_2F_1\left(\frac{1}{2}, \frac{2d}{d-1}; \frac{3}{2}; \sin^2 \chi_e\right) \sin \chi_e \right). \quad (5.14)$$

For $d = 2$, this result reduces consistently to Eq. (5.4), recovering the four-dimensional case. One observes that $H(\chi)$ is an odd function, while $N(\chi)$ is not even unless $H(\chi_c) = 0$. A further analysis of the metric solution reveals results analogous to those found in the four-dimensional case, leading to several parallel conclusions. First, there exists a potential \mathbb{Z}_2 symmetry between χ_c and χ_e , indicating a redundancy in characterizing the geometry through either root. There is a critical value χ_c satisfying $H(\chi_c^*) = 0$, at which the function $N(\chi)$ becomes even. The metrics corresponding to $\chi_c \in (0, \chi_c^*)$ and $\chi_c \in (\chi_c^*, \pi/2)$ are related by the coordinate reflection $\chi \rightarrow -\chi$. Second, from a geometric viewpoint, in higher dimensions the Euclidean spacetime contains two horizons, with the sphere radius attaining its minimum value m at $\chi = 0$, reminiscent of a wormhole throat. Finally, upon explicit computation, the Euclidean action takes the universal form

$$I_E = -\frac{1}{4}(\mathcal{A}_c + \mathcal{A}_e) = -\frac{\Omega_d}{4} \left(\frac{m^d}{(\cos \chi_c)^{2d/(d-1)}} + \frac{m^d}{(\cos \chi_e)^{2d/(d-1)}} \right). \quad (5.15)$$

It can be shown that, despite the increasing complexity in higher dimensions, the point $\chi_c = \chi_c^*$ remains a stationary point (a local maximum) of the I_E - χ_c curve, whereas $\chi_c = 0$ (or, equivalently, $\chi_c = \pi/2$) corresponds to another stationary point (a local minimum). The corresponding behaviors are illustrated in Fig. 8(a) and Fig. 8(b). This generalizes the four-dimensional result discussed previously: both cases exhibit the hidden \mathbb{Z}_2 symmetry and yield a Euclidean action proportional to the total horizon area, highlighting the universality of these general features extending beyond the four-dimensional case ($D = 4$ or $d = 2$).

6 Euclidean geometry as constrained instantons

As discussed earlier, the extended massive VCEG possesses two horizons, with conical singularities arising at both $\chi = \chi_c$ and $\chi = \chi_e$. In general, these singularities cannot be simultaneously eliminated; they are removed only when m attains its maximal value m^* , for which $\beta_c = \beta_e$. The resulting configuration is referred to as the critical VCEG. In contrast,

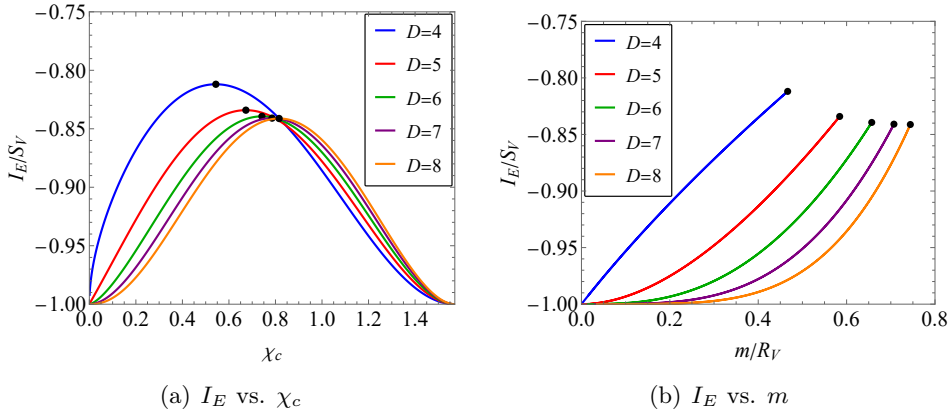


Figure 8. Euclidean action I_E/S_V as a function of (a) χ_c and (b) m/R_V in different spacetime dimensions. Black dots indicate the critical configurations at $\chi_c = \chi_c^*$ and $m = m^*$.

the massless VCEG features only a single horizon. For $m \neq 0$ and $m \neq m^*$, the extended VCEG inevitably exhibits conical singularities, indicating that the configuration is not in thermal equilibrium. This closely parallels the situation in pure dS spacetime and the SdS black hole. The Euclidean SdS geometry likewise possesses two horizons associated with conical singularities, which can be simultaneously removed only when the black hole mass reaches its maximal value—corresponding to the Nariai geometry—where the two horizons coincide. Conversely, the massless limit of the SdS black hole reduces to pure dS spacetime, featuring a single horizon. These parallels suggest a close analogy between the extended VCEG and the Euclidean SdS black hole.

For extended VCEGs with mass in the range $0 < m < m^*$, the conical singularities render the Euclidean solutions non-regular, and, as seen in Fig. 8(a), they do not correspond to stationary points of the Euclidean action. These solutions can thus be interpreted as configurations at a fixed mass parameter m , that is, regarded as a mass-constrained instanton in close analogy with the treatment of the SdS black hole discussed in Refs. [39, 40]. Although the massless VCEG corresponds to the minimum of the Euclidean action, massive configurations may still be generated through quantum fluctuations. From the perspective of the thermodynamic ensemble, extended VCEGs with different mass parameters contribute to the partition function as constrained instantons, and their contributions should be summed over.

6.1 Constrained instantons in gravity

An essential element in our analysis is the method of constrained instantons [35, 36], originally developed in quantum field theory. Recently, this idea has been further explored in the context of gravitational theories [37, 38]. Constrained instanton configurations are particularly significant because, although they are not saddle points for the Euclidean action in the conventional sense, they still contribute to nonperturbative processes in quantum gravity.

In Einstein gravity with a fixed-volume constraint, the extended massive VCEG provides a concrete realization of such a constrained instanton.

We begin with the path integral formulation of quantum gravity, where the fundamental variable is the metric field g_{ab} . The partition function can be rewritten as,

$$\begin{aligned}\mathcal{Z} &= \int [\mathcal{D}g] \exp(-I_E[g]) \\ &= \int d\mu \int [\mathcal{D}g] \delta(\mathcal{C}[g] - \mu) \exp(-I_E[g]) \\ &= \int d\alpha \int d\mu \int [\mathcal{D}g] \exp(-I_E[g] + \alpha(\mathcal{C}[g] - \mu)).\end{aligned}\tag{6.1}$$

In the second line, we have inserted a constraint $\mathcal{C}[g]$ together with an auxiliary integration variable μ ; this step is harmless. In the third line, the Dirac delta function has been represented as an integral of α along the imaginary axis. The resulting effective action now depends on the gravitational field g_{ab} as well as on the additional parameters α and μ . The corresponding equations follow from varying the exponent with respect to g_{ab} and α ,

$$\frac{\delta I_E[g]}{\delta g_{ab}} + \alpha \frac{\delta \mathcal{C}[g]}{\delta g_{ab}} = 0, \quad \mathcal{C}[g] = \mu.\tag{6.2}$$

These equations define the gravitational field equations under the constraint, where α acts as a Lagrange multiplier. If one further varies with respect to μ , the condition $\alpha = 0$ arises, which restores the first equation to the ordinary, unconstrained Einstein equations. However, if we ignore the variation with respect to μ and solve only Eq. (6.2), we obtain a family of solutions $g_{ab}^{(\mu)}$ and corresponding multipliers $\alpha^{(\mu)}$. Whenever $\alpha^{(\mu)} \neq 0$, the resulting geometry is referred to as a constrained instanton. Within the saddle-point approximation, substituting these constrained instantons back into the path integral yields

$$\mathcal{Z} \simeq \int d\mu \exp\left(-I_E[g^{(\mu)}]\right).\tag{6.3}$$

Thus, the partition function is expressed as a sum over geometries labeled by the constraint parameter μ . In general, the extrema of $I_E[g^{(\mu)}]$ with respect to μ correspond to the ordinary (unconstrained) saddle points, which are characterized by $\alpha^{(\mu)} = 0$. Inspired by this, one can infer that the extrema along the curve of the Euclidean action $I_E[g^{(\mu)}]$ as a function of μ correspond to genuine saddle points, while the constrained instantons play the role of intermediate configurations connecting these saddles.

It is worth emphasizing that, from the above discussion, the action (2.1) can indeed be regarded as the Einstein-Hilbert action subject to a constraint, with the Lagrange multiplier μ identified with the fixed spatial volume V . In this sense, the corresponding massless and critical VCEGs are constrained instantons of Einstein gravity. However, our primary focus is on the action of Einstein gravity with a volume constraint, which serves as the fundamental action to be evaluated in the path integral. Within this framework, the massless and critical VCEGs correspond to genuine saddle points of the constrained action, whereas the massive

VCEGs with $m \neq m^*$ are naturally interpreted as constrained gravitational instantons. We will elaborate on this point in detail below.

For a generic extended massive VCEG with $m \neq m^*$, although the unavoidable conical singularities prevent it from being a true saddle point of the action (2.1), such a geometry should be interpreted as a constrained instanton with fixed mass constant. Specifically, following the discussion of the SdS black hole in Refs. [39, 40], we divide the extended VCEG into two manifolds by introducing a timelike hypersurface at $\chi = \chi_0$, such that the two conical singularities at $\chi = \chi_c$ and $\chi = \chi_e$ are separated onto the two manifolds. On this timelike hypersurface, we fix the extrinsic curvature \mathcal{K} as the constraint condition, which is equivalent to fixing the mass parameter. In this way, the conical singularities on the two manifolds can be removed by assigning appropriate periods to the Euclidean time coordinate on each manifold. Thus, the extended massive VCEG with $m \neq m^*$ is interpreted as a mass-constrained gravitational instanton, and the resulting contribution to the action is determined by the Gibbons-Hawking-York term on the horizons. Using the calculation in Eq. (4.5), one finds that the first term vanishes in the horizon limit, while the second term gives the area term. This result is also consistent with our expression (5.15).

From another viewpoint, the ensemble-averaged theory of black holes, it is also natural to include configurations with conical singularities in the path integral. As discussed in Refs. [54–57], for a given ensemble temperature, a Euclidean black hole typically possesses conical singularities unless the ensemble temperature exactly matches the Hawking temperature. In this case, the Euclidean action becomes a function of the horizon radius r_h , and the stationary points of this action with respect to r_h correspond precisely to regular (singularity-free) geometries. Moreover, when the ensemble average is taken, the Hawking-Page transition for the SAdS black hole, as well as the small-large black hole transition for the Reissner-Nordström AdS black hole, naturally emerge as semiclassical approximations in the regime where the system size is much larger than the Planck length. Beyond the semiclassical limit, the system becomes a superposition of different geometries, and the averaged quantities deviate from standard black hole thermodynamics. In our case, for the extended massive VCEG, there generally exist unavoidable conical singularities under a fixed ensemble temperature, located respectively on the two horizons. From the ensemble-averaged perspective, although such configurations possess conical defects, they should still contribute to the gravitational path integral. Furthermore, as discussed above, the dominant contribution comes from the $m = 0$ configuration, which corresponds to a stable point.

Therefore, whether viewed from the perspective of constrained instantons or from the ensemble-averaged theory, the inclusion of these constrained instanton solutions in the semiclassical path integral is well justified. In analogy with the SdS case, we may identify the constraint parameter μ with the ratio M/M^* , whose range is $[0, 1]$. This choice is motivated by the SdS case and is intended to facilitate a direct comparison with the analysis in Ref. [40]. Still, a supplementary remark is in order. In the present treatment, we have assumed that, when μ is treated as the integration variable, the integrand is dominated solely by the exponential term, while the prefactor is treated as constant, as in Eq. (6.3). In general, this

prefactor receives contributions from fluctuations and zero modes. Even so, we expect that as a conceptual and approximate description of the instanton contribution, the expression in Eq. (6.3) provides a reasonable approximation.

6.2 Ensemble interpretation and quantum decay rate

As discussed before, both the gravitational instantons and the true saddle points are included in the partition function. The saddle points correspond to the extended VCEGs with $m = 0$ and $m = m^*$, where the former represents the Euclidean minimum and the latter corresponds to the maximum of the action. The gravitational instanton can then be regarded as an intermediate configuration connecting these two extrema. Therefore, in the absence of quantum effects, the geometry with $m = 0$ is classically stable. the geometry with $m = 0$ is classically stable. However, once quantum fluctuations are taken into account, a decay process may occur.

First, let us consider the contribution of the extended VCEG to the partition function. Since the integration is over the constraint parameter $\mu = M/M^*$ and the Euclidean action (5.15) depends on μ in a rather complicated manner, the resulting integral cannot be evaluated in analytic expression. To further address the difficulty of evaluating the integral, it is reasonable to adopt an approximate approach. As a first step, let us analyze the behavior of the Euclidean action I_E in the regime of small mass constant M . To clarify this behavior, let us take $\chi_c = \frac{\pi}{2} - \epsilon^{d-1}$, where ϵ is a small dimensionless parameter. Using the condition $N(\chi_e) = 0$, we find $\chi_e = -\frac{4}{d-1}\epsilon^4 + o(\epsilon^4)$. With the aid of the volume constraint (5.14) and the Euclidean action (5.15), we then obtain

$$\frac{m}{R_V} = \epsilon^2 - \frac{3d+1}{12(d-1)}\epsilon^{2d} + o(\epsilon^{2d}), \quad \frac{I_E}{S_V} = 1 - \frac{1}{4}d\epsilon^{2d-2} + o(\epsilon^{2d-2}), \quad (6.4)$$

where S_V is defined as one quarter of the area of a d -sphere with radius R_V , i.e. $S_V = \Omega_d R_V^d/4$. Noting that $m^{d-1} = 16\pi M/(d\Omega_d)$, eliminating ϵ gives

$$\frac{I_E}{S_V} = -1 + \frac{1}{4}d\left(\frac{m}{R_V}\right)^{d-1} + o\left(\left(\frac{m}{R_V}\right)^{d-1}\right) = -1 + \frac{4\pi}{\Omega_d} \frac{M}{R_V^{d-1}} + o\left(\frac{M}{R_V^{d-1}}\right), \quad (6.5)$$

which suggests that, at leading order, a linear relation arises between I_E and M . Accordingly, we adopt the following approximate relation

$$I_E \approx -S_V + \frac{S_V - S^*}{M^*}M = -S_V + \Delta S \mu, \quad \Delta S \equiv S_V - S^*, \quad (6.6)$$

where the entropy S^* represents that of the critical extended VCEG, and the entropy difference ΔS is positive. The corresponding linear approximation (dashed lines) and the exact results (solid lines) are shown in Fig. 9. Under this approximation, the corresponding partition function can be evaluated as

$$\mathcal{Z} \simeq \int d\mu \exp\left(-I_E[g^{(\mu)}]\right) \approx \int_0^1 d\mu e^{S_V - \Delta S \mu} = \frac{e^{S_V}}{\Delta S} (1 - e^{-\Delta S}). \quad (6.7)$$

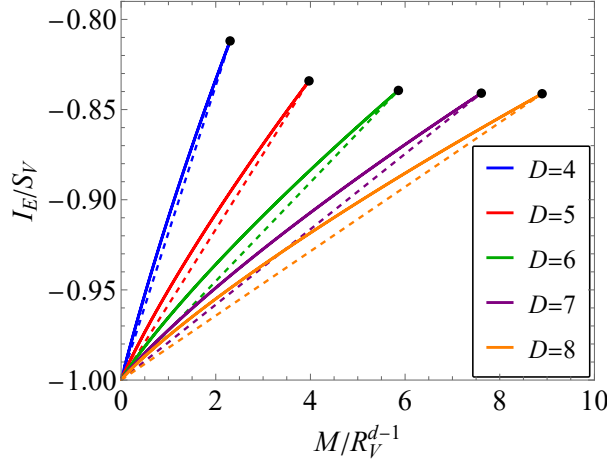


Figure 9. Relations of the Euclidean action with M in different spacetime dimension. Black dots indicate the critical configurations at $\chi_c = \chi_c^*$, $m = m^*$ and $M = M^*$.

It is evident that the partition function depends only on the entropies associated with the two limiting configurations, namely extended massless VCEG and critical extended VCEG. We note that for $m = m^*$, the corresponding $\chi_c = \chi_c^*$ and $\chi_e = \chi_e^*$ are determined as the roots of $H(\chi) = 0$, and therefore do not depend on the volume radius R_V . From the volume constraint (5.14), it follows that $m^* \propto R_V$, with a proportionality factor that depends on the spacetime dimension. Restoring the Planck length in the expression for the entropy, one finds $S^* \propto (R_V/\ell_p)^d$ and $\Delta S \propto (R_V/\ell_p)^d$, similar to S_V , though with different numerical coefficients. Consequently, the partition function (6.7) depends only on the dimensionless ratio R_V/ℓ_p and on the spacetime dimension D .

When the ratio R_V/ℓ_p becomes either much smaller or much larger than unity, the partition function can be approximated as

$$\mathcal{Z} \approx \begin{cases} e^{S_V} \left(1 - \frac{1}{2} \Delta S\right), & \text{for } R_V/\ell_p \ll 1, \\ e^{S_V} \frac{1}{\Delta S}, & \text{for } R_V/\ell_p \gg 1. \end{cases} \quad (6.8)$$

It is evident that when the radius R_V is much larger than the Planck length ℓ_p , the partition function acquires only a multiplicative correction factor. In contrast, when $R_V \ll \ell_p$, gravitational effects become significant and S_V itself becomes small. In this regime, one can further expand

$$e^{S_V} \left(1 - \frac{1}{2} \Delta S + \mathcal{O}(\Delta S^2)\right) \approx e^{S_V - \frac{1}{2} \Delta S + \mathcal{O}(\Delta S^2)} = e^{\frac{1}{2}(S_V + S^*) + \mathcal{O}(\Delta S^2)}, \quad (6.9)$$

indicating that the effective entropy is corrected to the mean value of the two entropies corresponding to $m = 0$ and $m = m^*$ configurations. This indirectly indicates that the saddle-point approximation ceases to be reliable in this regime, as nearly all configurations contribute with comparable weight, a manifestation of strong quantum fluctuations. Returning to the unapproximated expression of the partition function, Eq. (6.7), we note that the entropies of

extended VCEGs are smaller than S_V and larger than S^* , resulting in an effective entropy $\log \mathcal{Z}$ that is smaller than S_V . Consequently, as R_V/ℓ_p decreases (i.e., as quantum fluctuations become increasingly significant), the entropy of the gravitational system drops below S_V and approaches the lower bound $(S_V + S^*)/2$. Equivalently, this entropy reduction can be interpreted as an increase in the effective gravitational coupling G_{eff} under a fixed area law. Taking ℓ_p as the reference energy scale, this implies that at higher energies (smaller R_V), the effective coupling G_{eff} becomes larger.

Below, we briefly consider the decay probability from the massless VCEG to a extended massive VCEG, which can be approximately expressed as

$$\Gamma \approx M^* \int_0^1 d\mu e^{-\Delta S \mu^{d-1}} = \frac{M^*}{\Delta S} (1 - e^{-\Delta S}). \quad (6.10)$$

In the weak-gravity regime, where $R_V/\ell_p \gg 1$, one finds

$$\Gamma \approx M^* \frac{1}{\Delta S} = \frac{M^*}{S_V - S^*} = \# \frac{1}{R_V}, \quad (6.11)$$

where " $\#$ " denotes a dimensionless coefficient independent of R_V , which can be explicitly determined from the expressions of S_V , M^* and S^* . Since the temperature scales as $T \propto 1/R_V$ (with λm^2 treated as dimensionless), the decay rate in this limit is therefore proportional to the temperature.

In comparison with the analysis of SdS spacetime in Ref. [40], the extended VCEG exhibits strikingly similar features. As shown in Eq. (6.5), the Euclidean action exhibits a similar functional dependence on the mass constant M at leading order, and in the weak-gravity limit the decay rate is likewise proportional to the temperature. While the SdS spacetime reflects the influence of a cosmological constant, the extended VCEG corresponds to a gravitational configuration constrained by a fixed volume. This analogy indicates that the volume constraint plays a role similar to that of the cosmological constant, leading to comparable physical properties.

7 Conclusion and discussion

We have examined the Euclidean action and partition function of gravity under a fixed-volume constraint. This work extends the analysis of Ref. [27], in which the dominant saddle corresponds to a spherically symmetric configuration with a vanishing mass function. We have constructed constrained gravitational instantons with nonzero mass parameters (massive VCEGs) and evaluated their contributions to the Euclidean action. By incorporating these massive VCEGs, we clarify how the volume constraint shapes the space of admissible gravitational configurations and determines their relative weights in the ensemble.

Within the covariant phase space framework, as discussed in the Supplemental Material of Ref. [27], we review that even under a fixed volume constraint, configurations satisfying the

Hamiltonian and momentum constraints contribute to the action solely through horizon and boundary terms: the horizon accounts for the Wald entropy, while the boundary contributes to the energy. Consequently, for geometries without boundaries, the action in general relativity is universally determined by the horizon area, with the total energy vanishing. This observation reinforces the interpretation that the partition function encodes the dimension of the Hilbert space, with the relevant degrees of freedom effectively localized on the horizon. This picture is reminiscent of the holographic principle. In the case of the massless VCEG, the Euclidean action reduces entirely to one quarter of the horizon area, a result similar to that of pure dS space.

We obtained the VCEG for a nonzero mass constant. Although it contains both a boundary at $r = m$, the ADM Hamiltonian remains zero, and the Euclidean action continues to be determined by the horizon area. When the mass parameter is nonzero, the VCEG can be further analytically extended, in which case the geometry no longer possesses a boundary but instead contains two horizons. Each of these horizons exhibits a conical singularity, and it is generally impossible to choose a single period of the Euclidean time that simultaneously removes both singularities, except for the critical case specified by $m = m^*$ (i.e., the critical extended VCEG). Therefore, the unextended VCEG can be regarded as the portion of the extended VCEG with $\chi \geq 0$, corresponding to a manifold with boundary. For the extended VCEG, the Euclidean action is given by one quarter of the sum of the areas of the two horizons, which is consistent with the results for the SdS black hole [40]. Moreover, the following properties are also analogous to those of the SdS black hole: as shown in Eq. (6.5), when the mass constant M is treated as a small parameter, the subleading term of the Euclidean action is linear in M ; and in the classical limit the corresponding decay rate is proportional to the temperature T (as shown in Eq. (6.11)).

From a topological and geometrical perspective, the massless VCEG and Euclidean dS static patch are analogous, both being topologically equivalent to \mathbb{S}^{d+2} . In the case of nonzero mass, the extended massive VCEG and the Euclidean SdS black hole each contain two horizons, which may exhibit conical singularities. In general, it is not possible to simultaneously remove both singularities. Only when the mass parameter of the extended massive VCEG reaches its maximal value, corresponding to the maximal mass of the Euclidean SdS black hole, do the geometries correspond to the critical extended VCEG and the Nariai geometry, respectively. In this case, after smoothing out the conical singularities, the topology of both geometries becomes $\mathbb{S}^2 \times \mathbb{S}^d$.

Before proceeding further, it is important to note that the above discussion applies to dimensions $D \geq 4$. The case of $D = 3$ is special, and the corresponding results are presented in Appendix A. As shown there, in three dimensions neither the massless nor the massive VCEG requires any further extension, and the geometry is defined over the radial interval $r \in [0, r_c]$. For any value of the mass parameter m , VCEG contains only a single horizon, and its topology is that of \mathbb{S}^3 . These features closely parallel those of the three-dimensional Euclidean SdS black hole. Moreover, just as Euclidean black hole, the contribution of the VCEG to the Euclidean action is determined solely by the area term. Thus, in $D = 3$, the

two systems display a clear similarity.

Both topological and Euclidean action analyses reveal that the extended VCEG closely parallels the SdS black hole. These results suggest that the volume constraint effectively plays a role analogous to that of a cosmological constant. It is instructive to consider the Euclidean actions of the two cases. More specifically, the volume constraint and the cosmological constant terms can be written as

$$-\lambda(\tau)\sqrt{\gamma}, \quad \frac{1}{8\pi}\Lambda\sqrt{g} = \frac{1}{8\pi}\Lambda N\sqrt{\gamma}, \quad (7.1)$$

where we have omitted the volume term V , as it does not affect the equations of motion for the gravitational field. First, the VCEG arises for $\lambda < 0$, while the dS geometry corresponds to $\Lambda > 0$. Therefore, the two share the same overall sign convention, a similarity that ensures the resulting geometry is as compact as possible. Second, the difference in the lapse function between the two cases implies that the corresponding gravitational solutions are not identical. Typically, for stationary solutions, the lapse function depends on the coordinate r . However, this difference does not play a crucial role in the present discussion, particularly in the analysis of the topology and the Euclidean action. Nevertheless, achieving a complete equivalence between the two terms in Eq. (7.1) would require promoting the cosmological constant to a spacetime-dependent field $\Lambda(x)$, whose effect would precisely cancel that of the lapse function. Such a result may be realized from the viewpoint of symmetry breaking, where introducing an additional effective potential for $\Lambda(x)$ allows it to acquire the desired functional form.

Upon reviewing the Euclidean action (2.1), it is clear that it consists solely of contributions from Einstein gravity and the volume constraint. The instanton solution of the constraint, in turn, reveals properties characteristic of the SdS black hole and wormholes. This observation naturally leads to the speculation that the dS-like behavior of our universe could, in principle, arise from an effective volume constraint rather than from a fundamental cosmological constant.

Acknowledgments

We are grateful to Xiang-Cheng Meng for valuable help and useful discussions. This work was supported by the National Natural Science Foundation of China (Grants No. 12475055, No. 12405073, and No. 12247101), the Fundamental Research Funds for the Central Universities (Grant No. lzujbky-2025-jdzx07), the Natural Science Foundation of Gansu Province (No. 22JR5RA389, No.25JRRA799), and Natural Science Foundation of Tianjin (No. 25JCQNJC01920).

A Special Case: three dimensions

Although many of the conclusions remain similar in higher dimensions, for instance the appearance of cutoff regions in the spacetime due to mass excitations, the situation in three dimensions is markedly different. In analogy with Sec. 2, one may also discuss the TOV equation in the three-dimensional case. Here, however, we focus on the configuration in which the

energy density $\rho(r)$ vanishes, as this corresponds to the solution of the field equations obtained by varying the action (2.1). Concretely, the components of the energy-momentum tensor are given by $T_{ab} = -\rho(r)n_a n_b + p(r)\gamma_{ab}$, where

$$\rho(r) = 0, \quad p(r) = \frac{m-1}{4\pi(r_c^2 - r^2)}. \quad (\text{A.1})$$

The corresponding gravitational solution takes the form,

$$N(r) = \frac{4\pi\lambda}{m-1} (r_c^2 - r^2), \quad M = \frac{m}{8}, \quad (\text{A.2})$$

leading to the metric,

$$ds^2 = \frac{16\pi^2\lambda^2}{(1-m)^2} (r_c^2 - r^2)^2 d\tau^2 + \frac{1}{1-m} dr^2 + r^2 d\phi^2. \quad (\text{A.3})$$

The radial metric component g_{rr} is independent of r , but it is required to be positive, which implies that the mass parameter m must be smaller than 1. In analyzing the solution, we have assumed in advance that $N(r) > 0$, which in turn requires $\lambda < 0$, consistent with the case of $D \geq 4$. However, unlike in higher dimensions, the radial coordinate here ranges over $[0, r_c]$. It is important to note that as $r \rightarrow 0$, if one naively sets the periodicity of ϕ to 2π , a conical singularity would arise at $r = 0$. To avoid this singularity, the periodicity of ϕ must instead be chosen as $2\pi(1-m)^{-1/2}$. At this stage, the spatial volume constraint can be expressed as

$$V = \frac{1}{1-m} \pi r_c^2. \quad (\text{A.4})$$

Accordingly, the relation between m and r_c dictated by the volume constraint is shown in Fig. 10. In contrast to the case of $d \geq 4$, here r_c is a monotonically decreasing function of m , and the relation between r_c and m does not asymptotically approach the identity line at large m . Furthermore, under the volume constraint, the functional profiles of $N(r)$ for different values of m are displayed in Fig. 11. These plots illustrate that varying m effectively corresponds to changing the cutoff radius r_c .

Considering the contribution of the metric (A.3) to the action, we readily obtain

$$I_E = -\frac{1}{2\sqrt{1-m}} \pi r_c = -\frac{1}{2} \pi R_V, \quad (\text{A.5})$$

where R_V is defined through the volume $V = \pi R_V^2$. It can be seen that, in three dimensions, a nonzero value of m is in fact trivial. Indeed, by rescaling the coordinates as $r \rightarrow r\sqrt{1-m}$ and $\phi \rightarrow \phi/\sqrt{1-m}$, the metric (A.3) is brought back to the case with $m = 0$.

References

[1] S. W. Hawking, *Particle Creation by Black Holes*, Commun. Math. Phys. **43**, 199 (1975), [erratum: Commun. Math. Phys. **46**, 206 (1976)].

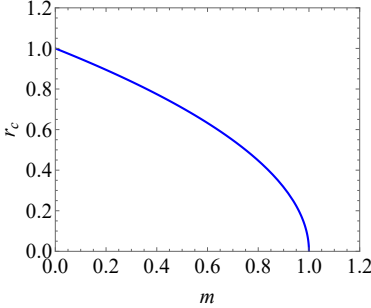


Figure 10. Relation between the mass parameter m and r_c at fixed volume. The volume is chosen to be that of a unit ball in two dimensions, $V = \pi$.

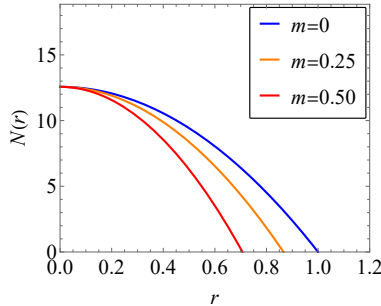


Figure 11. Functional profiles of $N(r)$ at fixed volume $V = \pi$. The blue, orange, and red curves correspond to $m = 0$ ($r_c = 1$), $m = 0.25$ ($r_c \approx 0.93$), and $m = 0.50$ ($r_c \approx 0.84$), respectively. Throughout the plot, the parameter λ is fixed at -1 .

- [2] J. D. Bekenstein, *Black holes and entropy*, Phys. Rev. D **7**, 2333 (1973).
- [3] S. W. Hawking, *Black Holes and Thermodynamics*, Phys. Rev. D **13**, 191 (1976).
- [4] J. B. Hartle and S. W. Hawking, *Path Integral Derivation of Black Hole Radiance*, Phys. Rev. D **13**, 2188 (1976).
- [5] G. W. Gibbons and S. W. Hawking, *Action Integrals and Partition Functions in Quantum Gravity*, Phys. Rev. D **15**, 2752 (1977).
- [6] J. D. Bekenstein, *Black holes and the second law*, Lett. Nuovo Cim. **4**, 737 (1972).
- [7] J. M. Bardeen, B. Carter and S. W. Hawking, *The Four laws of black hole mechanics*, Commun. Math. Phys. **31**, 161 (1973).
- [8] J. D. Bekenstein, *Generalized second law of thermodynamics in black hole physics*, Phys. Rev. D **9**, 3292 (1974).
- [9] S. W. Hawking and D. N. Page, *Thermodynamics of Black Holes in anti-De Sitter Space*, Commun. Math. Phys. **87**, 577 (1983).
- [10] A. Chamblin, R. Emparan, C. V. Johnson and R. C. Myers, *Charged AdS black holes and catastrophic holography*, Phys. Rev. D **60**, 064018 (1999), [arXiv:hep-th/9902170 [hep-th]].
- [11] A. Chamblin, R. Emparan, C. V. Johnson and R. C. Myers, *Holography, thermodynamics and*

fluctuations of charged AdS black holes, Phys. Rev. D **60**, 104026 (1999), [arXiv:hep-th/9904197 [hep-th]].

[12] D. Kubiznak and R. B. Mann, *P-V criticality of charged AdS black holes*, JHEP **07**, 033 (2012), [arXiv:1205.0559 [hep-th]].

[13] G. 't Hooft, *Dimensional reduction in quantum gravity*, Conf. Proc. C **930308**, 284 (1993), [arXiv:gr-qc/9310026 [gr-qc]].

[14] L. Susskind, *The World as a hologram*, J. Math. Phys. **36**, 6377 (1995), [arXiv:hep-th/9409089 [hep-th]].

[15] J. M. Maldacena, *The Large N limit of superconformal field theories and supergravity*, Adv. Theor. Math. Phys. **2**, 231 (1998), [arXiv:hep-th/9711200 [hep-th]].

[16] E. Witten, *Anti de Sitter space and holography*, Adv. Theor. Math. Phys. **2**, 253 (1998), [arXiv:hep-th/9802150 [hep-th]].

[17] G. Hayward, *Euclidean action and the thermodynamics of manifolds without boundary*, Phys. Rev. D **41**, 3248 (1990).

[18] B. F. Whiting and J. W. York, Jr., *Action Principle and Partition Function for the Gravitational Field in Black Hole Topologies*, Phys. Rev. Lett. **61**, 1336 (1988).

[19] B. Banihashemi and T. Jacobson, *Thermodynamic ensembles with cosmological horizons*, JHEP **07**, 042 (2022), [arXiv:2204.05324 [hep-th]].

[20] S. P. Wu, Y. X. Liu and S. W. Wei, *Generalized Free Energy Landscapes from Iyer-Wald Formalism*, [arXiv:2504.00503 [hep-th]].

[21] W. Fischler, *Taking de Sitter seriously*, Talk given at “Role of scaling laws in physics and biology” (celebrating the 60th birthday of Geoffrey West), Santa Fe (2000).

[22] T. Banks, *Cosmological breaking of supersymmetry?*, Int. J. Mod. Phys. A **16**, 910 (2001), [arXiv:hep-th/0007146 [hep-th]].

[23] A. Strominger, *The dS / CFT correspondence*, JHEP **10**, 034 (2001), [arXiv:hep-th/0106113 [hep-th]].

[24] T. Banks and W. Fischler, *Holographic cosmology 3.0*, Phys. Scripta T **117**, 56 (2005), [arXiv:hep-th/0310288 [hep-th]].

[25] X. Dong, E. Silverstein and G. Torroba, *De Sitter Holography and Entanglement Entropy*, JHEP **07**, 050 (2018), [arXiv:1804.08623 [hep-th]].

[26] J. C. Chang, S. He, Y. X. Liu and L. Zhao, *Holographic $T\bar{T}$ deformation of the entanglement entropy in $(A)dS_3/CFT_2$* , Phys. Rev. D **112**, 026013 (2025), [arXiv:2409.08198 [hep-th]].

[27] T. Jacobson and M. R. Visser, *Partition Function for a Volume of Space*, Phys. Rev. Lett. **130**, 221501 (2023), [arXiv:2212.10607 [hep-th]].

[28] M. Lu and R. B. Mann, *Lagrangian Partition Functions Subject to a Fixed Spatial Volume Constraint in the Lovelock Theory*, Entropy **26**, 291 (2024), [arXiv:2402.14235 [hep-th]].

[29] A. Tavlayan and B. Tekin, *Partition function of a volume of space in a higher curvature theory*, Phys. Rev. D **108**, L041902 (2023), [arXiv:2307.14210 [hep-th]].

[30] R. M. Wald, *Black hole entropy is the Noether charge*, Phys. Rev. D **48**, R3427 (1993), [arXiv:gr-qc/9307038 [gr-qc]].

[31] R. C. Tolman, *Static solutions of Einstein's field equations for spheres of fluid*, Phys. Rev. **55**, 364 (1939).

[32] R. F. C. Vessot, et al., *Test of Relativistic Gravitation with a Space-Borne Hydrogen Maser*, Phys. Rev. Lett. **45**, 2081 (1980).

[33] J. Ponce de Leon and N. Cruz, *Hydrostatic equilibrium of a perfect fluid sphere with exterior higher dimensional Schwarzschild space-time*, Gen. Rel. Grav. **32**, 1207 (2000), [arXiv:gr-qc/0207050 [gr-qc]].

[34] J. Pleyer, *Zero Values of the TOV Equation*, [arXiv:2411.15264 [gr-qc]].

[35] I. Affleck, *On Constrained Instantons*, Nucl. Phys. B **191**, 429 (1981).

[36] Y. Frishman and S. Yankielowicz, *Large Order Behavior of Perturbation Theory and Mass Terms*, Phys. Rev. D **19**, 540 (1979).

[37] J. Cotler and K. Jensen, *Gravitational Constrained Instantons*, Phys. Rev. D **104**, 081501 (2021), [arXiv:2010.02241 [hep-th]].

[38] J. Cotler and K. Jensen, *Wormholes and black hole microstates in AdS/CFT*, JHEP **09**, 001 (2021), [arXiv:2104.00601 [hep-th]].

[39] P. Draper and S. Farkas, *de Sitter black holes as constrained states in the Euclidean path integral*, Phys. Rev. D **105**, 126022 (2022), [arXiv:2203.02426 [hep-th]].

[40] E. K. Morvan, J. P. van der Schaar and M. R. Visser, *On the Euclidean action of de Sitter black holes and constrained instantons*, SciPost Phys. **14**, 022 (2023), [arXiv:2203.06155 [hep-th]].

[41] V. Iyer and R. M. Wald, *Some properties of Noether charge and a proposal for dynamical black hole entropy*, Phys. Rev. D **50**, 846 (1994), [arXiv:gr-qc/9403028 [gr-qc]].

[42] V. Iyer and R. M. Wald, *A Comparison of Noether charge and Euclidean methods for computing the entropy of stationary black holes*, Phys. Rev. D **52**, 4430 (1995), [arXiv:gr-qc/9503052 [gr-qc]].

[43] A. Seraj, *Conserved charges, surface degrees of freedom, and black hole entropy*, [arXiv:1603.02442 [hep-th]].

[44] G. Compère, *Advanced Lectures on General Relativity*, Lect. Notes Phys. **952**, 150 (2019) Springer, Cham, 2019.

[45] D. Harlow and J. Q. Wu, *Covariant phase space with boundaries*, JHEP **10**, 146 (2020), [arXiv:1906.08616 [hep-th]].

[46] W. Guo, X. Guo, M. Li, Z. Mou and H. Zhang, *Equivalence of Noether charge and Hilbert action boundary term formulas for the black hole entropy in $F(Rab_{cd})$ gravity theory*, Phys. Rev. D **110**, 064071 (2024), [arXiv:2406.15138 [hep-th]].

[47] W. Guo, X. Guo, X. Lan, H. Zhang and W. Zhang, *Background subtraction method is not only much simpler, but also as applicable as the covariant counterterm method*, Phys. Rev. D **111**, 084088 (2025), [arXiv:2501.08214 [hep-th]].

- [48] G. Barnich and F. Del Monte, *Introduction to Classical Gauge Field Theory and to Batalin-Vilkovisky Quantization*, [arXiv:1810.00442 [hep-th]].
- [49] R. Ruzziconi, *Asymptotic Symmetries in the Gauge Fixing Approach and the BMS Group*, PoS **Modave2019**, 003 (2020), [arXiv:1910.08367 [hep-th]].
- [50] D. V. Fursaev and S. N. Solodukhin, *On the description of the Riemannian geometry in the presence of conical defects*, Phys. Rev. D **52**, 2133 (1995), [arXiv:hep-th/9501127 [hep-th]].
- [51] S. N. Solodukhin, *The Conical singularity and quantum corrections to entropy of black hole*, Phys. Rev. D **51**, 609 (1995), [arXiv:hep-th/9407001 [hep-th]].
- [52] S. N. Solodukhin, *Entanglement entropy of black holes*, Living Rev. Rel. **14**, 8 (2011), [arXiv:1104.3712 [hep-th]].
- [53] R. Li and J. Wang, *Generalized free energy landscape of a black hole phase transition*, Phys. Rev. D **106**, 106015 (2022), [arXiv:2206.02623 [hep-th]].
- [54] P. Cheng, Y. X. Liu and S. W. Wei, *Black hole thermodynamics from an ensemble-averaged theory*, Phys. Rev. D **111**, 4 (2025), [arXiv:2408.09500 [gr-qc]].
- [55] P. Cheng, J. Pan, H. Xu and S. J. Yang, *Thermodynamics of the Kerr-AdS black hole from an ensemble-averaged theory*, Eur. Phys. J. C **85**, 423 (2025), [arXiv:2410.23006 [hep-th]].
- [56] M. S. Ali, C. Fairoos, C. L. A. Rizwan, T. K. Safir and P. Cheng, *Thermodynamics of Einstein-Gauss-Bonnet Black Holes and Ensemble-averaged Theory*, [arXiv:2411.07147 [gr-qc]].
- [57] Y. Q. Liu, H. W. Yu and P. Cheng, *Quantum-corrected black hole thermodynamics from the gravitational path integral*, [arXiv:2506.15261 [hep-th]].